

RECURRENCE QUANTIFICATION ANALYSIS OF SYSTEM SIGNALS FOR DETECTING TOOL WEAR AND CHATTER IN TURNING

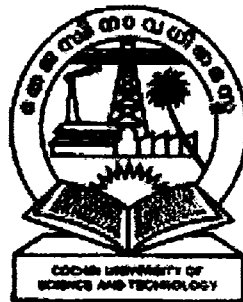
A thesis

submitted in partial fulfillment of the degree of

DOCTOR OF PHILOSOPHY

by

RAJESH V.G.

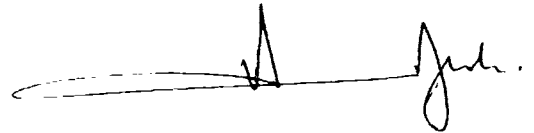


**DIVISION OF MECHANICAL ENGINEERING, SCHOOL OF ENGINEERING
COCHIN UNIVERSITY OF SCIENCE AND TECHNOLOGY, KERALA
INDIA
JANUARY, 2008**

Declaration

I hereby declare that the work presented in this thesis entitled "Recurrence Quantification Analysis of System Signals for Detecting Tool and Chatter in Turning" is based on the original work done by me under the supervision and guidance of Dr. Narayanan Namboothiri V.N., Faculty, Division of Mechanical Engineering, School of Engineering, CUSAT. No part of this thesis has been presented for any other degree from any other institution.

Thrikkakara
23.01.2008



Rajesh V.G.

Certificate

This is to certify that the thesis entitled "Recurrence Quantification Analysis of System Signals for Detecting Tool and Chatter in Turning" is a report of the original work done by Sri. Rajesh V.G., under my supervision and guidance in the School of Engineering. No part of this thesis has been presented for any other degree from any other institution.



Thrikkakara
23.01.2008

Dr. Narayanan Namboothiri V.N.
Supervising Guide,
Faculty,
Division of Mechanical Engineering,
School of Engineering,

Acknowledgements

This work could not be realized without the help and support of many people.

First, I wish to express my gratitude to the Director, Institute of Human Resources Development, Thiruvananthapuram, India for deputing me for this Ph.D programme.

I would like to thank Dr. P.S. Sreejith, Principal and HOD of the Division of Mechanical Engineering, School of Engineering, Cochin University of Science and Technology, India for providing me the resources and facilities to carryout this thesis work.

I am extremely grateful to Dr. Narayanan Namboothiri V.N., my supervising guide, for providing me with the opportunity to work in the field of nonlinear dynamics; who has encouraged and inspired me with new ideas and fruitful discussions. I am indebted to him for allowing me the opportunity to pursue my Ph.D. programme under him in the university.

I am grateful to the members of the Research Committee of the School of Engineering, for their kind suggestions at various stages of this work.

I would like to gratefully acknowledge the useful and stimulating discussions with Prof. Charles L. Webber, Jr., Loyola University Chicago, at various stages of this work; who has enriched this work with new ideas and suggestions.

I would like to thank the All India Council for Technical Education, New Delhi for their generosity in permitting me to use the equipments and software made available for the sponsored project under RPS scheme No. PLB1/6723/05.

Further I sincerely thank my friends and colleagues in the labs where I have worked; Smt. Usha Nair, Sri. Radhakrishnan P.M., Sri. Jacob Elias, Smt. Bindu M. Krishna, Sri. Anslam Raj, Sri. Sabeer Muhammed and Sri. Shouri P.V. for sharing their ideas and for the fruitful co-operation.

I gratefully thank Dr. V.P.N. Nampoori, Director, International School of Photonics for allowing me to audit classes in his department and for discussion and support regarding the presentation part of the work.

I would like to thank Prof. Mani T.K. and Prof. Rajesh M.V. of the Model Engineering College, Cochin for assisting me in the design and fabrication of both the sensors used in the experiments.

Thanks are also due to Sri. Babu Varghese of the Machine Shop for his help in performing the experimental testing in the machine shop and for providing all supports. I also thank Sri. Job and Joben for their technical assistances in the making of the sensors.

My special thanks goes to Reshmy for her endless and manifold support and encouragement. I am truly grateful to my Sooryan for his patience with me.

Finally I would like to dedicate this thesis to my mother and to the memories of my great father.

Abstract

In this thesis, the applications of the recurrence quantification analysis in metal cutting operation in a lathe, with specific objective to detect tool wear and chatter, are presented.

This study is based on the discovery that process dynamics in a lathe is low dimensional chaotic. It implies that the machine dynamics is controllable using principles of chaos theory. This understanding is to revolutionize the feature extraction methodologies used in condition monitoring systems as conventional linear methods or models are incapable of capturing the critical and strange behaviors associated with the metal cutting process.

As sensor based approaches provide an automated and cost effective way to monitor and control, an efficient feature extraction methodology based on nonlinear time series analysis is much more demanding. The task here is more complex when the information has to be deduced solely from sensor signals since traditional methods do not address the issue of how to treat noise present in real-world processes and its non-stationarity. In an effort to get over these two issues to the maximum possible, this thesis adopts the recurrence quantification analysis methodology in the study since this feature extraction technique is found to be robust against noise and stationarity in the signals.

The work consists of two different sets of experiments in a lathe; set-1 and set-2. The experiment, set-1, study the influence of tool wear on the RQA variables whereas the

set-2 is carried out to identify the sensitive RQA variables to machine tool chatter followed by its validation in actual cutting. To obtain the bounds of the spectrum of the significant RQA variable values, in set-1, a fresh tool and a worn tool are used for cutting. The first part of the set-2 experiments uses a stepped shaft in order to create chatter at a known location. And the second part uses a conical section having a uniform taper along the axis for creating chatter to onset at some distance from the smaller end by gradually increasing the depth of cut while keeping the spindle speed and feed rate constant.

The study concludes by revealing the dependence of certain RQA variables; percent determinism, percent recurrence and entropy, to tool wear and chatter unambiguously. The performances of the results establish this methodology to be viable for detection of tool wear and chatter in metal cutting operation in a lathe. The key reason is that the dynamics of the system under study have been nonlinear and the recurrence quantification analysis can characterize them adequately.

This work establishes that principles and practice of machining can be considerably benefited and advanced from using nonlinear dynamics and chaos theory.

Table of contents

DECLARATION	I
CERTIFICATE	II
ACKNOWLEDGEMENTS	III
ABSTRACT	V
TABLE OF CONTENTS	VII
LIST OF TABLES	X
LIST OF FIGURES	XI
ABBREVIATIONS	XIII
CHAPTER 1 - INTRODUCTION	1
1.1 Motivation	4
1.2 Aim of the thesis	4
1.3 Thesis outline	5
CHAPTER 2 - BACKGROUND LITERATURE REVIEW	6
2.1 TCM research	6
2.2 Chatter research	15
2.3 Nonlinear dynamics of cutting process	18
CHAPTER 3 - SIGNAL ANALYSIS FRAMEWORK	24
3.1 Nonlinear time series analysis	24
3.2 Methods and implementation	28

3.2.1	Phase Space Reconstruction – Taken’s Embedding Theorem	28
3.2.2	Selecting the time delay –Average mutual information method	30
3.2.3	Selecting the embedding dimension – False nearest neighbors method	33
3.3	Time series analysis based on recurrence plots	36
3.3.1	Distance and recurrence matrices	37
3.3.2	Threshold radius	39
3.3.3	Structures in recurrence plots	40
3.3.4	Measures of complexity–Recurrence quantification analysis	44
3.3.5	Selection of the threshold radius	47
3.3.6	Episodic recurrences	49
3.4	Summary	51
CHAPTER 4 - RESEARCH METHODOLOGY		52
4.1	Procedure	52
4.2	Mann-Whitney U test	54
CHAPTER 5 - EXPERIMENTAL SETUP AND DATA ACQUISITIONS		56
5.1	Description of the machine tool	56
5.2	Details of the test specimen	56
5.3	Specifications of tool insert	58
5.4	Description of the data acquisition system-sensors	58
5.4.1	Current sensor	58
5.4.2	Vibration sensor	59
5.5	NI DAQ components	61
5.6	ADXL 150 accelerometer	61
5.7	Block schematic of current sensor	63
5.8	Summary	64

CHAPTER 6 - EXPERIMENTS AND RESULTS	65
6.1 SECTION ONE	66
6.1.1 Experiments and data acquisition	67
6.1.2 Data analysis	68
6.1.2.1 Recurrence quantification analysis	68
6.1.2.2 Surrogate data test	72
6.1.2.3 Mann-Whitney U test	75
6.1.2.4 RQA episodic test	75
6.1.2.5 Observations	78
6.2 SECTION TWO	79
6.2.1 Experiment set 2 – Part 1	80
6.2.1.1 Experiments and data acquisition	80
6.2.1.2 Data analysis	82
6.2.2 Experiment set 2-Part 2	85
6.2.2.1 Experiments and data acquisition	85
6.2.2.2 Data analysis	86
6.2.2.3 Observations	89
Chapter 7 - SUMMARY, BENEFITS AND FUTURE DIRECTIONS	90
7.1 Summary	91
7.2 Benefits	92
7.3 Contributions	93
7.4 Future directions	93
7.5 Conclusion	93
LIST OF PAPERS SUBMITTED BASED ON THIS THESIS	94
REFERENCES	96
APPENDIX	
1 Mathematical Construction of the Recurrence Matrix	108
2 Mann-Whitney U test – Example Problem	113

List of Tables

Table No.	Table Caption	Page No.
3.1	Comparison of linear and nonlinear signal processing techniques.	27
3.2	Typical patterns in RPs and their meanings	43
6.1	Phase space reconstruction parameters obtained by AMI and FNN	68
6.2	Phase space reconstruction parameters actually used in the analysis	70
6.3	Calculated values for the threshold ϵ	70
6.4	Chosen values for the threshold ϵ	70
6.5	RQA values of current and vibration signals for system using fresh and worn tool.	73
6.6	RQA values of current and vibration signals for system using fresh and worn tool, using both intact and randomized data sets	74
6.7	RQA Variables – Mann-Whitney U test results	75
6.8	RQA input parameters for Part-1 experimental time series	82
6.9	RQA input parameters for Part-2 experimental time series	86

List of Figures

Figure No.	Figure Caption	Page No.
3.1	Typical examples of recurrence plots	38
3.2	Three commonly used norms for the neighborhood with the same radius around a point	39
3.3	Representation of a hypothetical system in higher dimensional phase space with a splay of points	40
3.4	A diagonal line in a RP corresponds with a section of a trajectory (dashed) which stays within an ϵ -tube around another section (solid).	42
3.5	Methods for selecting the proper radius parameter for recurrence analysis of a sample data	48
3.6	Windowed recurrence analysis of EMG signal.	50
4.1	Research Methodology	53
5.1	Test Configuration for Experiment Set-1	57

5.2	Test configuration for Experiment Set-2	57
5.3	Data acquisition flow diagram for the current sensor.	59
5.4	Turning operation showing positioning of accelerometer on tool holder	59
5.5	Data acquisition flow diagram for the current sensor.	60
5.6	NI DAQ components	61
5.7	ADXL 150 accelerometer details	63
5.8	Block schematic of the voltage and current measurement setup	63
6.1	Delay Vs. AMI plot for worn tool – Current sensor data	69
6.2	Embedding dimension Vs. FNN plot for worn tool – Current sensor data	69
6.3	Recurrence plots of current and vibration signals data for system using fresh and worn tool.	73
6.4	Episodic recurrence analysis of test signals	77
6.5	Part-1 experimental time series	81
6.6	RQA results for Part-1 experimental time series	83
6.6	RQA results for Part-1 experimental time series	84
6.7	RQA variables - Set-2 experimental time series	87
6.7	RQA variables - Set-2 experimental time series	88

Abbreviations

%DET	Percent Determinism
%LAM	Percent Laminarity
%REC	Percent Recurrence
<i>DM</i>	Distance Matrix
ENT	Entropy
LMAX	Linemax
LOI	Line of Identity
NTSA	Nonlinear Time Series Analysis
<i>RM</i>	Recurrence Matrix
RP	Recurrence Plot
RPs	Recurrence Plots
RQA	Recurrence Quantification Analysis
TCM	Tool Condition Monitoring
TND	Trend
TT	Trapping Time

Chapter 1 - Introduction

Machining is one of the most ubiquitous operations in a manufacturing system. About 70% of products produced in modern manufacturing enterprises are known to undergo a machining process at some stage of their production. The outcome of this process often determines the quality and the operational performance of products emerging from a manufacturing enterprise system.

The phenomenon of tool wear and machine tool chatter has long been a matter of concern to industry because of their detrimental effects on the efficient operation of any machining process on tool life, part quality and machine utilization. In any metal cutting operation, the cutting tool is subjected to continuous wear due to its intermittent or constant contact with the work piece material. One of the key factors that affect production optimization and surface quality of the work piece is the state of cutting tool characterized by the tool wear. To change a tool when worn requires on-line monitoring. The reason for this is primarily because tool wear is a complex phenomenon that manifests itself in different and varied ways. It leads to catastrophic tool failures increasing the machine tool downtime. Similarly, machine tool chatter is another serious issue, as it limits the maximum processing speed for machine-cutting applications. Chatter promotes excessive machining forces and tool wear, tool failure, and scrap parts due to unacceptable surface finish and possible damage to the machine tool system.

In the past, machinists have attempted to avoid chatter through trial and error. Monitoring of tool wear had been done manually by using a combination of sight and

sound by human operators. Accuracy of these methods largely depends on experience as well as workmanship. However, these methods for controlling and monitoring manufacturing operations, mainly based on the experience and craftsmanship of the machinists, are fast becoming obsolete. These days, the effort is more critical than it once was because of the shortage of skilled workers, higher process speeds, increases in precision machining, a need to lower downtime, and the trend toward machine tool enclosures. When fewer workers must do more tasks, automation becomes essential and tool monitors and chatter control are the key elements in the automation package. For these reasons, on-line real-time quality control schemes incorporating identification of tool wear or chatter in metal cutting produce significant cost savings for manufacturers.

Given the trend for globalization of markets, it is imperative that these schemes be robust and help producing good and consistent quality products. Building on this understanding, substantial progress has already been made in tool developments, in-process real time monitoring and control of tools and in chatter research. These studies lead to the fundamental understanding of tool wear and chatter mechanisms and a number of methods have been suggested for their detection and control. Linear as well as non-linear methods of analysis were used by researchers in their studies.

Later, chaos theory based modeling has led to the finding that metal cutting exhibits low dimensional chaos under normal operating conditions. The main implication of this result is that the dynamics are controllable using the chaos theory. This realization is having a fairly large impact on the classical views concerning the dynamics of metal cutting which spurred interest and led to attractor-based fractal analysis applying nonlinear methodologies. The twin assumptions that the dynamics of a given process or system is chaotic and the sensor signals are not highly contaminated underlie the application of a fractal analysis. If these assumptions are not valid, the values of parameters/coefficients calculated using fractal analysis have little relevance to the characteristics of sensor signals.

A mechanical system signal is by nature non-stationary and is usually corrupted with dynamic or measurement noise which necessitates pre-processing. Signal analysis of such a data, therefore, demands an analysis methodology that is tested to be robust against these two important attributes. Moreover, most methods of nonlinear data analysis methodologies need rather long data series.

In the last decade, a new method based on nonlinear data analysis has become popular: Recurrence Plots (RPs). Recurrence is a fundamental property of dissipative dynamical systems. Although small perturbations of such a system cause exponential divergence of its state, after some time the system will come back to a state that is arbitrarily close to a former state and pass through a small evolution. RPs visualize such recurrent behavior of dynamical systems. Practitioners of this method have found its relevance for short, noisy and non-stationary data. These features are indeed the crucial advantage of RPs. As deduction of information by visually examining the RPs is more subjective, it was then developed into Recurrence Quantification Analysis (RQA). This quantifies the number and duration of recurrences of a dynamical system presented by its phase space trajectory. The Features extracted from the RPs by RQA, contain information about the system. These features are called the RQA variables and it can be used for characterizing a dynamical system.

Since the RQA methodology is found to provide useful information even for short, non-stationary and noisy data, this analytical tool can be ideally suited for the characterization of complexity in a mechanical system which exhibits chaotic behavior. The thesis work, therefore, adopts the RQA methodology for the analysis of captured sensor signals, and investigates the tool wear and chatter conditions produced during turning in a lathe. The work attempts to characterize the system signals generated, first by identifying the significant RQA variables, and then by studying their sensitivity to tool wear and chatter.

1.1 Motivation

The motivation for this work came primarily from two quarters-non-stationary and noise contaminated nature of sensor data due to mechanical systems, and applications of RP-based methods of nonlinear time series analysis which addresses these issues.

Moreover, the RQA can output useful information from even a short data set, which makes it an attractive feature extraction methodology suitable for deployment in the monitoring of real-time cutting process.

1.2 Aim of the Thesis

The all-embracing goal of machining dynamics studies that uses any fractal estimation methodology has been to establish a relation between tool wear or machine failure with the dimensions of the attractor of the dynamics. The practical use is of course to link these values to monitoring and diagnostics of the cutting process using an appropriate neural network. It is to note that all of these studies were initiated by the discovery that metal cutting exhibits low dimensional chaos.

Interestingly none of the studies did explore the recurrent behavior of the dynamical system. Clearly there is valuable information hidden in such behavior of the system, and the primary aim of this thesis is to make use of a versatile signal processing methodology called RQA to emphasize and extract this information contained in machining dynamics. Sensor signal characteristics have been a guiding star throughout the work. More specifically, the aims of this thesis are to:

- To study the nonlinear characteristics of turning in a lathe
- To investigate the applications of RP-based approaches in characterizing the dynamics of turning

- To study and experimentally validate the applicability of RQA methodology in detecting tool wear and chatter in turning.

1.3 Thesis Outline

Chapter 1 introduces the problem at hand and defines the aim of the thesis

Chapter 2 contains a review of background literature on tool condition monitoring, chatter and nonlinear dynamics of cutting process.

Chapter 3 describes methods for nonlinear time series analysis and introduces dynamical system theory with specific reference to RP based approaches, within the context of signal processing.

Chapter 4 presents the research methodology adopted in the thesis

Chapter 5 describes the experimental setup and the data acquisition systems used in the experiments

Chapter 6 presents the experiments and discusses the results

Chapter 7 contains conclusions with pointers for future work

Chapter 2 – Background Literature Review

This chapter sets the scene for up-coming sections. It is basically an assessment of the present state-of-the-art of the wide and complex fields of machine tool chatter and tool condition monitoring (TCM) and control. Also, this chapter separately reviews what has been done in the past in the area of nonlinear dynamics of metal cutting process.

2.1 *TCM Research*

Considerable research has been conducted in the area of tool monitoring and control due to the fact that tool failure represents about 20% of machine tool down-time and that tool wear negatively impacts the work quality in the context of dimensions, finish, and surface quality.

Vision is a suitable technique to evaluate tool wear in a laboratory setting although attempts have been made to use this technique on shop floors as a direct measure system. Among the technology bottlenecks of this measurement is the illumination issue. Different light sources such as coherent light from a 0.8 mm diameter laser [1] and halogen lamp [2] have been used along with various other light configurations, including a two-light arrangement [3], to record tool wear images. The sensor to be used on-line must survive the harsh machining environment under chips and atomized coolant [4]. Most of the image techniques are limited to 2D; however a 3D measurement system using a pair of stereo imaging was developed by Karthik et al. [5]

to identify the crater wear volume. However, this method is useful only for crater wear, which does not occur for all cutting conditions.

The forces developed in machining are affected by the tool geometry. As the tool gets worn the geometry changes, thereby impacting the cutting forces. Early attempts found that the feed and radial forces are more sensitive to tool wear than the cutting forces [6, 7]. The radial force component was reported to be most sensitive to nose wear, with the feed force and the radial components affected by flank wear [8]. Similarly flank wear was observed to correlate with the feed and cutting force components [9]. Force ratios can also be used to predict tool wear since they present a certain pattern as the tool wears [10]. The feed force to cutting force ratio was found to be sensitive to flank wear [9].

During cutting, the work piece undergoes considerable plastic deformation associated with the generation of acoustic emission (AE). Progressive tool wear affects the cutting zone with a change in the AE signal. Due to its high frequency feature (1 kHz to 1000 kHz, far beyond machine tool resonance), AE is generally found to be more sensitive to tool wear than cutting forces [11]. Strong correlation of the AE RMS to tool wear was presented [12] where statistical features like mean, variance and the coefficients of RMS were related to tool wear. The variance was the most sensitive parameter, showing the largest amplitude at the end of tool life. Other AE features like ring-down, rise time, event duration, frequency and event rate, as well as time series coefficients [13] have also been correlated to tool wear and chipping [14]. However the lack of physical understanding of the AE signal and its sensitivity to sensor location and cutting parameters remain difficult issues for the application of this technology.

The temperature in the cutting zone can change as the tool wears due to change in the tool geometry and its ability to cut; therefore, the use of temperature was suggested to monitor the tool state. As an early attempt, Moshref [15] predicted the tool wear area

using an empirical relation of temperature difference to wear difference ratio correlated with cutting time. However, the temperature measured on the back of the cutting tool is not the true temperature on the cutting zone. Recently, Choudhary et al.[16] experimentally correlated the relation between the flank wear and cutting zone temperature in turning where the temperature sensor was the natural formed thermocouple between the tool and the work piece. In this case, only the average temperature in the cutting zone is sensed. Another possibility is to measure the temperature by thermo images from the cutting zone. However, in this case the chip which carries approximately 90% of the energy dissipated during cutting, will dominate the intensity of radiation.

The embedded thermocouples and thermo images are the indirect measurements that can be used to predict the temperature distribution if a proper heat conduction model is used. Derrico [17] assumed a simple relation between the measured temperature with an embedded thermocouple and the tool face temperature as a scaling factor and a propagation delay. Lin [18] measured the temperature outside the cutting zone in milling by an infrared pyrometer and estimated the interface temperature by an inverse finite element method. This method is affected for the internal properties of the work piece. Lima et. al [19] performed a numerical simulation to estimate the cutting temperature using a three-dimensional inverse heat conduction technique. However this technique was not implemented in a real cutting process.

Vibrations are produced by cyclic variations in the dynamic components of the cutting forces. Mechanical vibrations generally result from periodic wave motions. The nature of the vibration signal arising from the metal cutting process is such that it incorporates facets of free, forced, periodic and random types of vibration. Direct measurement of vibration is difficult to achieve because its determining characteristic feature, the vibration mode is frequency dependent. Hence, related parameters such as the rate at

which dynamic forces change per unit time (acceleration) are measured and the characteristics of the vibration derived from the patterns obtained.

Dimla [20] presents a detailed investigation of progressive tool wear results obtained during a metal turning operation. Dry cutting was conducted using P15 and P25 tool inserts from which the three principal components of the vibration signal was obtained. A tool life picture was constructed in both time and frequency domains for each vibration component using three tool wear form measurements (flank, nose and notch). The accumulative sum total power of the spectra signal was used to interpret the time domain characteristics while spectra and contour plots described the frequency characteristics. The accumulative power features were ineffective in gradual tool wear monitoring but reasonable at chipping/fracture detection. Spectra plots for the tool characteristics at first contact (i.e. when tool was new and therefore sharp) to those describing the severely worn tool characteristics (or the occasional chipping/failure modes) were produced. The two types of tool inserts used showed slight differences in their active tool lives as a result of the hot hardness effect of the coatings, but the investigation indicated that the amount of wear and its form was reliant more on the prevailing cutting conditions.

El-Wardany et al. [21] investigated the use of vibration signature characteristics in on-line drill wear monitoring and breakage. Vibration signature features sensitive to the tool wear were identified in time and frequency domains. Experimental results showed that the kurtosis values increased drastically with drill breakage while frequency analysis revealed sharp peaks indicating drill breakage. By combining both techniques, it was possible to devise an effective drill monitoring system.

Yao et al. [22] investigated detection and estimation of groove wear at the minor cutting edge of the tool by monitoring vibration signatures. A multivariate time series analysis was carried out on the recorded vibration signals using a combination of autoregressive

moving averages and some explicit functions. The dispersion analysis showed that the thrust cutting force and vibration were sensitive to the length of groove wear with two peaks: one at a very low frequency < 200 Hz and the other at a high frequency ≥ 10 kHz.

Dan and Mathew [23] employed a discrete modeling method called data dependent system to correlate vibration signals to cutting tool wear. The implementation of this method involved the isolation of the vibration signal deemed to be most sensitive to tool wear. Obtained results showed some variation in the amount of vibration energy within a specific frequency band that was consistently observed regardless of cutting parameter. The application of spectral analysis to the acceleration signals revealed a linear relationship between the cutting speed and tool wear showing that vibration signals were sensitive to tool wear.

Rotberg et al. [24,25] were interested in mechanical signature analysis (vibration) for tool state prediction during interrupted cutting. In Rotberg et al. [24] the emphasis was on the milling tool entry and exit conditions. Face milling experiments were conducted and the ensuing flank and crater wear measured. Detailed signal processing of the recorded signals was carried out. Wear curves, average envelop at three points of tool life (sharp, part worn, worn) and spectral descriptions of the three wear phases were established. Inspection of the plots indicated that the vibration signal was a suitable indicator of tool wear as it demonstrated considerable change during tool life. Rotberg et al. [25] focused on tool wear monitoring using vibration as the principal signal. The analysis was performed using two basic models characterized by their signal features: low frequency and high frequency. Experiments were conducted to validate these models utilizing recorded acceleration signal features. They concluded that their analysis showed certain peculiar and universally occurring features from the vibration signals that could be harnessed in developing a TCMS as it correlated well with tool wear.

Jiang et al. [26] using a purposely-built test-rig was able to investigate the effects of vibration in the cutting and feed directions on the cutting tool. Using fixed cutting conditions, tests were conducted utilizing plane-faced P10 tool inserts with each cut lasting 10 minutes in a single pass. During the time of active tool engagement, the wear on the tool gradually increased until it catastrophically failed. The recorded signals were post-processed and power spectra density (PSD) of the vibration signals produced. Three distinctive regions identified on the PSD could be divided into the frequency ranges: up to 100 Hz, 117–510 Hz and 510–1000 Hz, from which they performed an in-process method of tool wear monitoring based on frequency band energy analysis. They concluded that their experimental investigations provided sufficient evidence that vibration signals were sensitive to tool wear states.

The inter-relationship between vibration signals and the cutting forces determines the dynamic nature of the cutting process, making the utilization of these process parameters attractive in the development of TCMs [20]. The static behavior is governed solely by the cutting forces and momentum (or torsion of the tool holder). The dynamic behavior on the other hand embodies vibration and certain aspects of the dynamic cutting force.

Zhang et al. [27] used a Hall effect sensor to measure the current supplied to the spindle motor drive of a vertical NC miller together with the cutting forces. The relationship between the measured motor current and the milling torque was developed by modeling the acquired motor current and torque. Computer algorithms were developed to track the waveforms, rate of peak change and the relative eccentricities of the modeled relation. They concluded that cutter breakages were reliably diagnosed with motor current measurements than force/torque measurements. Constantinides and Bennett [28] obtained the spindle motor power from a vertical milling machine and attempted to analyze the PSD, the moving average, running mean and the accumulative sum power to estimate tool wear. They concluded that spectral energy fluctuations of

the spindle motor power were linearly related to the tool wear rate but was also affected by the cutting conditions and tool geometry. Shaft power, cutting forces, torque and motor current are all related to each other, originating from, and depending entirely on one another. It suffices therefore to measure just one of these.

Xiaoli et al.[29] estimated the feed cutting force with the aid of an inexpensive current sensor installed on the ac servomotor of a computerized numerical control turning centre and is used to monitor tool wear condition. To achieve this, the feed drive system is modeled, using neuro-fuzzy techniques, to provide the framework for estimating the feed cutting force based on the feed motor current measured. Functional dependence of the feed cutting force on tool wear and cutting parameters were then expressed in the form of a difference equation relating variation in the feed cutting force to tool wear rate. The computerized system automatically compared successive feed cutting force estimates and determined the onset of accelerated tool wear in order to issue a request for tool replacement. Experimental results exhibit that the tool wear condition monitoring is effective and industrially applicable.

Different sensors used to detect wear and breakage in drilling, reaming, and tapping operations are listed by O'Donnell [30]. The torque signal has the most useful information to monitor these processes; however, the use of torque sensor is not always possible. Therefore O'Donnell [30] presented an experimental research in drilling with multiple sensor types and locations that include POWER, vibration and AE signals. The vibration and AE signals presented high levels of noise related to the manufacturing environment. The power signal presented the GREATEST sensitivity to variations in the tool performance and the LEAST sensitivity to noise.

In their work, Karali et al.[31] applied a multilayer neural network with back propagation algorithm to predict the average flank wear of a high speed steel drill bit for drilling on a mild steel work piece. Drilling experiments were carried out over a wide range of cutting

conditions and the effects of drill wear, cutting conditions (speed, drill diameter, feed-rate) on the spindle motor current have been investigated. The performance of the trained neural network was tested for new cutting conditions, and found to be in very good agreement to the experimentally determined drill wear values. The accuracy of the prediction of drill wear using neural network was found to be better than that using regression model.

Other varieties of sensors have also been employed in various attempts at tool wear prediction, monitoring or process parameter measurements in a metal cutting process. They include optical methods, stress/strain measurement, methods based on measuring the work piece dimension, surface finish quality measurement, and ultrasonic methods.

Martin et al. [32] summarized in a review that, amongst the optical methods to have been proposed for tool wear measurements were, laser measurement of the surface finish, photodiodes used in reflected light measurement from the cutting edge, and fiber optic photocell for reflectance measurement of worn and unworn areas of the tool flank. Clearly, none of these methods are applicable in a TCMS scenario as in-process tool wear measurement is more difficult to achieve. Other attempts based on optical techniques for tool wear sensing are listed in Ref. [33]. Kurada and Bradley [34] present a review of the basic principle, instrumentation and various image processing schemes involved in the development of a vision based TCMS. Oguamanam et al. [35], Kassim et al. [36] and Cuppini et al. [37] carried out implementation of this method. Shiraishi [38] through many years of research and experience cited that optical based methods for TCM are riddled with high inaccuracies and are therefore unreliable.

Noori-Khajavi and Komanduri [39] used amongst other sensors, strain sensors in their study of the correlation of process parameters to drill wear. The recorded signals were analyzed in both time and frequency domains but meaningful correlation of the drill wear could only be achieved in the frequency domain. Zhou et al. [40] proposed to

monitor the stresses acting in a cutting edge during a machining process in order to predict tool spontaneous failure. By monitoring the risk factor defined as a ratio of the instantaneous stresses, they reported that it was possible to predict spontaneous failures. Lee et al. [41] proposed another method based on stress analysis of three-dimensional loading. They combined FEA and detailed stress analysis of the cutting edges and tips of sharp and worn tools from which they concluded that it was possible to predict the mode and location of tool failure.

El-Gomayel and Bregger [42] proposed a method for tool wear monitoring based on measurements of work piece deviation. They employed two electromagnetic probes on opposite sides of the work piece such that electromagnetic waves could flow from the probe to the metal allowing accurate measurements of the work piece diameter. They concluded that though their model could measure minute tool wear, it could not quantify it (i.e. distinguish nose wear from flank wear).

Jetley and Gollajesse [43] proposed the magnetization of tool inserts and then, monitoring the magnetic field flux reduction as the tool wore. A preliminary investigative study involving the use of magnetized drills was devised and implemented in order to validate their methodology. They concluded that it was possible to accurately predict the end of tool life or fracture "on-line" by observing the magnetic flux, and the system was cost effective with potential for implementation in most metal cutting environments.

Abu-Zahra and Nayfeh [44] developed a normalized ultrasonic signal based method for in process tool wear monitoring for turning operations. A purposely-designed tool-holder accommodating the ultrasonic transducer was used to measure the gradual flank and nose wear forms. As the system developed required a specialized tool-holder, they conceded that commercialization would require a more versatile tool-transducer coupling to accommodate the various tool-holders and insert geometry.

A review of some of the methods that have been employed in TCMS [45], a discussion on the impact, industrial realizations, and future trends of machining process monitoring and control technologies [46] and the status of research and industrial applications of TCM [47] are detailed and can be found in these literatures.

The above survey suggest that, cutting forces (static and dynamic) and vibration(acceleration) are considered to be the most widely applicable parameters to tool wear, based on ease of harnessing and reliability. From the point of view of lowest cost, greatest sensitivity to tool performance and least sensitivity to noise, power signal is the best bet. Advances and increased sophistication in instrumentation technology employed for measuring these parameters make them viable, practical, easy to mount and have the quick response time needed to indicate changes for on-line monitoring.

In this work, two different sensors; a current sensor and an accelerometer are used to measure the lathe drive motor current and cutting tool vibrations respectively. These are found to be reliable, robust, inexpensive and easy to mount. Moreover, the current signal forms an input type signal whereas the vibration signals is an output type signal as far as the system consisting of lathe tool is considered.

2.2 Chatter Research

Chatter is a well known phenomenon, occurrence of which is undesired in manufacturing. It is characterized by noise, undulated surface finish, and machine vibration [48]. Chatter not only spoils the surface finish but also the dimensional accuracy, tool wear, surface integrity, and the cost of the manufacturing process since the chatter marks are difficult to remove. Aggressive machining conditions, in the sense of removing more metal rapidly, usually cause chatter. As accepted in the community, there are two groups of machine tool chatter: regenerative and non-regenerative. Regenerative chatter occurs due to the undulations on the earlier cut surface, and non-

regenerative chatter has to do with mode coupling among the existing modal oscillations.

Researchers such as Tlusty, Tobias, Stepan and many others have developed the fundamental knowledge of chatter, especially for the geometry of orthogonal cutting. As early in 1906, Taylor recognized the process limitations imposed by chatter, as well as the complexity in modeling its source, when he stated that chatter is the “most obscure and delicate of all problems facing the machinist” [49]. Later, work by Arnold proposed the negative damping effect as the source of chatter [50], while research by Tlusty and Tobias led to a fundamental understanding of regeneration of waviness, or the over cutting of a machined surface by a vibrating cutter, as a primary feedback mechanism for the growth of self-excited vibrations (or chatter) due to the modulation of the instantaneous chip thickness, cutting force variation, and subsequent tool vibration [51-55]. Tlusty and Tobias also described the mode coupling effect as a second chatter mechanism.

Efforts at modeling the process dynamics in order to select stable combinations of chip width, or axial depth of cut in peripheral milling operations, and spindle speed, can be loosely divided into a) analytical, b) experimental, and 3) numerical techniques [56-81]. The most common output of these simulations is the stability lobe diagram [51, 55, 56], a graphical tool which identifies the boundary between stable and unstable cutting zones in a two-dimensional map of the primary control parameters: chip width and spindle speed. These lobes allow for greater material removal while maintaining stability of the process at specific spindle speeds. However, there is little published experiment data to support this theory. Many researchers have opted not to experimentally explore the stability lobes since they generally occur at high spindle speeds that have not been obtainable or practical in the past. Here high is a relative term that is dependent upon the dynamic characteristics of the machine.

A significant amount of research has been devoted to automatic chatter detection. It is well known that the chatter frequency occurs near a dominant structural frequency. Thus the most common approach to chatter detection is to investigate the spectral density of a process signal and develop a threshold value that indicates chatter. Delio et al.[82] and Altintas and Chan [83] investigated sound pressure as the process signal. Tarn and Li [84] created threshold values for the spectrum and the standard deviation of thrust forces and torque signals in machining operations. It should be noted that the tooth-passing frequency contains significant energy and the process signal must be properly filtered if the tooth passing frequency is close to a dominant structural frequency.. These threshold algorithms require an empirically selected threshold value that will not be valid over a wide range of cutting conditions. A more general signal was proposed by Bailey et. al [85]. An accelerometer mounted close to the cutting region provides for the calculation of ratio called variance ratio to indicate the presence of chatter.

Li et. al [86] introduced a technique to identify both tool wear and chatter in turning a nickel-based super alloys. It used the coherence function between two crossed accelerations from the bending vibration of the tool shank. The value of the coherence function at the chatter frequency reached unity at the onset of chatter. Its values at the first natural frequencies of the tool shank approached unity in the severe tool wear stage. The results are interpreted using the analysis of the coherence function for a single input-two output model.

Soliman et al.[87] used the spindle drive current signals of a vertical milling machine for monitoring chatter. He conducted both simulations and experimental works and assessed the sensitivity of current signals to slight process instability. He defined a statistical indicator-R value, to evaluate sensitivity. His results show that current signals can reliably transmit chatter conditions.

2.3 *Nonlinear Dynamics of Cutting Process*

Since the 1970s revolutionary ideas of nonlinear science have led to vastly improved understanding of extremely complex and nonlinear physical systems in a wide range of diverse applications. Wide-ranging studies of non-linear dynamical systems as a framework for solving complicated problems in manufacturing resulted in the applications of nonlinear dynamics to understand, control and optimize mechanical manufacturing processes such as cutting, grinding and forming. Also in cutting we could learn much from the interdisciplinary works with mathematicians and physicists. The discovery that metal cutting exhibits low dimensional chaos [88] created a significant impact on views concerning the dynamics of metal cutting. This idea would suggest that a small amount of chaos may actually be good in machining, since it introduces many scales in the surface topology. The groups lead by Kumara and Grabec are active in this area. However, no explicit models of the cutting process based on chaos theory have been developed as yet. The theory however has lead to new applications of fractals and wavelets in monitoring and diagnostics of cutting process.

The dynamics of a cutting process are influenced by many interacting physical phenomena, such as material flow, deformation and fracture, friction, tool wear, vibration of the machine tool, etc. Furthermore, different material properties, tool geometry, and cutting parameters can lead to significantly different cutting dynamics. These are probably the main reasons for the lack of a reliable analytical description of the cutting process.

Earlier models for turning operation were developed on the assumption that its dynamics is linear. Later models assumed linear dynamics contaminated with additive noise. However these models were inadequate especially for global characterization of the turning dynamics; one should therefore resort to nonlinear modes. Doi & Kato [89] performed some beautiful experiments on establishing chatter as a time-delay problem and also presented one of the earliest nonlinear models. Also, Tobias [51] and Tlustý

[90] and others have considered nonlinearity in their studies. Before 1975-1980, nonlinear dynamics analysis mainly consisted of perturbation analysis and numerical simulation. Random-like motions were not considered, even though time records of cutting dynamics clearly showed unsteady oscillations [51]. Since the 1980s new concepts of modeling, measuring and controlling nonlinear dynamics in material processing have appeared. A friction model was used by Grabec [91, 92] in his pioneering paper on chaos in machining. The observation of the complex response from the nonlinear model of Grabec[91] has prompted the speculation that the dynamics of the turning operation may be chaotic . Preliminary studies on nonlinear modeling and the existence of primary and secondary chatter were conducted by Marui et al. [93], Gradisek et al. [94], Wiercigroch and Cheng [95], Warminski et al. [96,97], Litak et al. [98], Pratt and Nayfeh [99], Stepan and Kalmar-Nagy [100]. The corresponding experimental results, mostly on an orthogonal cutting process, have been discussed in several recent papers [101-103].

Studies of nonlinear phenomena in machine-tool operations involved three different approaches.

- (i) Measurement of nonlinear force-displacement behavior of cutting or forming tools.
- (ii) Model-based studies of bifurcations using parameter variation.
- (iii) Time-series analysis of dynamic data for system identification.

The fundamental origins of nonlinear dynamics in material processing usually involve nonlinear relations between stress and strain, or stress and temperature or chemical kinetics and solid-state reactions in the material. Other sources involve nonlinear geometry such as contact forces or tool-work piece separation. There is a long history of force measurements in the literature over the past century. Many of these data are based on an assumption of a steady process. Thus, in cutting-force measurements, the

speed and depth of cut are fixed and the average force is measured as a function of steady material speed and cutting depth. However, this begs the question as to the real dynamic nature of the process. In a dynamic process, what happens when the cutting depth instantaneously decreases? Does one follow the average-force-depth curve or is there an unloading path similar to elasto-plastic unloading? Average force measurements often filter out the dynamic nature of the process.

Even though the classical model of Tobias [51] with nonlinear cutting force is quite successful in predicting the onset of chatter [71], it cannot possibly account for all phenomena displayed in real cutting experiments. Single degree-of-freedom deterministic time-delay models have been insufficient so far to explain low-amplitude dynamics below the stability boundary. Also, real tools have multiple degrees of freedom. Kalmar-Nagy et al. [104] examined the coupling between multiple degree-of-freedom tool dynamics and the regenerative effect in order to see if the chatter instability criteria will permit low-level instabilities. It was shown that this mode-coupled non conservative cutting tool model including the regenerative effect (time delay) can produce an instability criterion that admits the unrealistic, low-level or zero chip thickness chatter.

In their studies, Oxley & Hastings [105] present steady-state forces as functions of chip thickness, as well as cutting velocity for carbon steel. For example, they measured a decrease of cutting force versus material flow velocity in steel. They also measured the cutting forces for different tool rake angles. These relations were used by Grabec [91,92] to propose a non-regenerative two-degree of freedom model for cutting that predicted chaotic dynamics. However, the force measurements themselves are quasi-steady and were taken to be single-valued functions of chip thickness and material flow velocity.

Bifurcation methodology looks for dramatic changes in the topology of the dynamic orbits, such as a jump from equilibrium to a limit cycle (Hopf bifurcation) or a doubling of the period of a limit cycle. The critical values of the control parameter at which the dynamics topology changes enable the researcher to connect the model behavior with experimental observation in the actual process. These studies also allow one to design controllers to suppress unwanted dynamics or to change a sub critical Hopf bifurcation into a supercritical one. The phase-space methodology also lends itself to new diagnostic tools, such as Poincaré maps, which can be used to look for changes in the process dynamics [106-107]. The limitations of the model-based bifurcation approach are that the models are usually overly simplistic and not based on fundamental physics. The use of bifurcation tools is most effective when the phase-space dimension is small, say, less than or equal to four.

The time-series analysis method has become popular in recent years to analyze many dynamic physical phenomena from ocean waves, heartbeats, lasers and machine-tool cutting [108]. This method is based on the use of a series of digitally sampled data, from which an orbit in a pseudo-M-dimensional phase space is constructed. One of the fundamental objectives of this method is to place a bound on the dimension of the underlying phase space from which the dynamic data were sampled. This can be done with several statistical methods, including fractal dimension, false nearest neighbors (FNN), Lyapunov exponents, wavelets and several others. However, if model-based analysis can be criticized for its simplistic models, then nonlinear time-series analysis can be criticized for its assumed generality. Although it can be used for a wide variety of applications, it contains no physics. It is dependent on the data alone. Thus the results may be sensitive to the signal-to-noise ratio of the source measurement, signal - filtering, the time delay of the sampling, the number of data points in the sampling and whether the sensor captures the essential dynamics of the process. One of the fundamental questions regarding the physics of cutting solid materials is the nature and origin of low-level vibrations in so-called normal or good machining. This is cutting

below the chatter threshold. Below this threshold, linear models predict no self-excited motion. Yet when cutting tools are instrumented, one can see random-like bursts of oscillations with a centre frequency near the tool natural frequency. Work by Johnson [106] has carefully shown that these vibrations are significantly above any machine noise in a lathe-turning operation. These observations have been done by several laboratories, and time-series methodology has been used to diagnose the data to determine whether the signals are random or deterministic chaos [109-112, 88, 113-118, 106]. These experiments and others (Bukkapatnam et al.) suggest that normal cutting operations may be naturally chaotic. This idea would suggest that a small amount of chaos may actually be good in machining, since it introduces many scales in the surface topology. However, in the paper, Gradisek et al [116] now disavow the chaos theory for cutting and claim that the vibrations are random noise. See also Wiercigroch & Cheng [95]. So this controversy remains about the random or deterministic chaos nature of the dynamics of normal cutting of materials.

At this juncture one may ask, what is the unique role of nonlinear analysis in the study of cutting and chatter? It has been known for some time how to predict the onset of chatter using linear theory [52,62]. The special tasks for nonlinear theory in cutting research include

- (i) predicting steady chatter amplitude,
- (ii) providing understanding of sub critical chatter,
- (iii) explaining pre-chatter low-level chaotic vibrations,
- (iv) predicting dynamic chip morphology,
- (v) providing new diagnostics for tool wear,
- (vi) determining control models for chatter suppression,
- (vii) providing clues to better surface precision and quality.

Certainly, many or all of these goals were the basis of traditional research methodology in machining. But the use of nonlinear theory acknowledges the essential dynamic character of material removable processes that in more classical theories were - filtered out. However, there is a need to integrate the different methods of research, such as bifurcation theory, cutting-force characterization and time-series analysis, before nonlinear dynamics modeling can be useful in practice.

In this thesis work a modest attempt is made to address two closely connected phenomena in metal cutting; provide a new methodology for detection of tool wear and chatter in metal cutting. The methodology stems from nonlinear time series analysis and is based on Recurrence Plots.

Chapter 3 – Signal Analysis Framework

The underlying assumption of many signal processing tools is that the signals are Gaussian, stationary, linear and have high signal to noise ratio. This chapter introduces the RQA methodology suitable for analyzing signals that do not fall into these categories.

3.1 Nonlinear Time Series Analysis

Many quantities in nature fluctuate in time. Examples are the stock market, the weather, seismic waves, sunspots, heartbeats, and plant and animal populations. Until recently it was assumed that such fluctuations are a consequence of random and unpredictable events. With the discovery of chaos, it has come to be understood that some of these cases may be a result of deterministic chaos and hence predictable in the short term and amenable to simple modeling. Many tests have been developed to determine whether a time series is random or chaotic, and if the latter, to quantify the chaos. A positive maximal Lyapunov exponent derived from the time series, expresses irregular deterministic behavior, which is termed chaotic [119- 121], whereas dynamical systems with solely non-positive exponents are usually referred to as regular. If chaos is

found, it may be possible to improve the short-term predictability and enhance understanding of the governing process of the dynamical system. We mean by talk of a 'dynamical system': a real-world system which changes over time.

While there is a long history of linear time series analysis, nonlinear methods have only just begun to reach maturity. When analyzing time series data with linear methods, there are certain standard procedures one can follow, moreover, the behavior may be completely described by a relatively small set of parameters. Linear methods interpret all regular structure in the data set, such as dominant frequency, as linear correlations. This means, in brief, that the intrinsic dynamics of the system are governed by the linear paradigm that small causes lead to small effects. Since linear equations can only lead to exponentially growing or periodically oscillating solutions, all irregular behavior of the system has to be attributed to some random external input to the system [122]. A brief comparison between linear and nonlinear methods [108] can be found in Table 3.1. Chaos theory has taught us that random input is not the only possible source of irregularity in a system's output: nonlinear, chaotic systems can produce very irregular data with purely deterministic equations of motion.

Now, Nonlinear Time Series Analysis (NTSA) is the study of the time series data with computational techniques sensitive to nonlinearity in the data. This was introduced by the theory of chaos to characterize the source complexity [122]. The NTSA theory offers tools that bridge the gap between experimentally observed irregular behavior and deterministic chaos theory. It enables us to extract characteristic quantities of a

particular dynamical system solely by analyzing the time course of one of its variables [122-124]. In theory, it would then be possible to collect temperature measurements in a particular city for a given period of time and employ nonlinear time series analysis to actually confirm the chaotic nature of the weather. Despite the fact that this idea is truly charming, its realization is not feasible quite so easily. In order to justify the calculation of characteristic quantities of the chaotic system, the time series must originate from a (i) stationary, (ii) deterministic system.

A deterministic dynamical system is one for which there is a rule, and, given sufficient knowledge of the current state of the system one can use the rule to predict future states; i.e. the future state x_{n+t} can be determined precisely from the current state x_n at any instance n for some value of $t > 0$, by applying the deterministic rule for the dynamical system. The other important requirement before attempting to do quantitative analysis is identification of stationarity of the dynamical system. Dynamical systems that are not stationary are exceedingly difficult to model from time series. Unless one has a priori knowledge of the structure of the underlying system, the number of parameters will greatly exceed the number of available data [125]. It may be noted here that the definition for stationarity is not the same as for linear systems: a linear system is said to be stationary if all its moments remain unchanged with time. A non-stationary system is defined as a one which is subject to temporal dependence based on some outside influence. If we extend our definition of the system to include all outside influences, the system is stationary.

Table 3.1. Comparison of linear and nonlinear signal processing techniques.

Linear signal processing	Nonlinear signal processing
Finding the signal:	Finding the signal:
Separate broadband noise from narrowband signal using spectral characteristics. Method: Matched filter in frequency domain.	Separate broadband signal from broadband noise using the deterministic nature of the signal. Method: Manifold decomposition or statistics on the attractor.
Finding the space:	Finding the space:
Use Fourier space methods to turn difference equations into algebraic forms.	Time lagged variables form coordinates for a reconstructed state space in m dimensions.
$x(t)$ is observed	$X(t) = [x(t), x(t + \tau), x(t + 2\tau), \dots, x(t + (m-1)\tau)]$
$X(f) = \sum x(t)e^{j2\pi ft}$ is used	where τ and m are determined by false nearest neighbors and average mutual information.
Classify the signal:	Classify the signal:
<ul style="list-style-type: none"> • Sharp spectral peaks • Resonant frequencies of the system 	<ul style="list-style-type: none"> • Lyapunov exponents • Fractal dimension measures • Unstable fixed points • Recurrence quantification • Statistical distribution of the attractor
Making models, predict:	Making models, predict:
$x(t+1) = \sum \alpha_k x(t-k)$	$X(t) \rightarrow X(t+1)$
Find parameters α_k consistent with invariant classifiers – location of spectral peaks.	$X(t+1) = F[X(t), a_1, a_2, \dots, a_p]$ Find parameters a_j consistent with invariant classifier – Lyapunov exponents, fractal dimensions.

3.2 Methods and Implementation

Let us suppose that we have a dynamical system which is both stationary and deterministic. To apply the nonlinear time series methods, the dynamics of the system are to be presented in a phase space. When the equations that govern process dynamics are not known, the phase space is reconstructed from a measured time series by using only one observation. The most basic step in this procedure is to rely on a time delayed embedding of the data, i.e. attractor reconstruction. For this purpose, we have to determine the proper embedding delay and embedding dimension. There exist two methods, developed in the framework of nonlinear time series analysis, that enable us to successfully perform these desired tasks. The average mutual information method [126] yields an estimate for the proper embedding delay, whereas the false nearest neighbor method [127] enables us to determine a proper embedding dimension.

In the following sub sections the methods of phase space reconstruction, average mutual information method and false nearest neighbors method are discussed.

3.2.1 Phase Space Reconstruction – Taken’s Embedding Theorem

The basic idea of the phase space reconstruction is that a signal contains information about unobserved state variables which can be used to predict the present state. Therefore, a scalar time series $\{x(j)\}$ may be used to construct a vector time series that is equivalent to the original dynamics from a topological point of view.

The problem of how to connect the phase space or state space vector of dynamical variables of the physical system to the time series measured in experiments was first addressed in 1980 by Packard et. al [128] who showed that it was possible to reconstruct a multidimensional state-space vector $X(i)$ by using time delays (or advances which we write as positive delays) with the measured, scalar time series, $\{x(j)\}$. Takens [129] and later Sauer et. al [130] put this idea on a mathematically sound footing by proving a theorem which forms the basis of the methodology of delays. They showed that the equivalent phase space trajectory preserves the topological structures of the original phase space trajectory. Due to this dynamical and topological equivalence, the characterization and prediction based on the reconstructed state space is as valid as if it was made in the true state space. The attractor so reconstructed can be characterized by a set of static and dynamic characteristics. The static characteristics describe the geometrical properties of the attractor whereas the dynamical characteristics describe the dynamical properties of nearby trajectories in phase space.

Thus, given a time series $\{x(j)\} = x(1), x(2), x(3), \dots, x(N)$ we define points $X(i)$ in an m -dimensional state space as

$$X(i) = [x(i), x(i+\tau), x(i+2\tau), \dots, x(i+(m-1)\tau)] \quad (1)$$

for $i = 1, 2, 3, \dots, N - (m-1)\tau$ where i are time indices, τ , a time delay or sometime referred to as embedding delay, and m is called the embedding dimension. Time evolution of

$X(i)$ is called a trajectory of the system, and the space, which this trajectory evolves in, is called the reconstructed phase space or simply, embedding space.

While the implementation of Eq. (1), the mathematical statement of Takens' Embedding theorem, should not pose a problem, the correct choice of proper embedding parameters τ and m is a somewhat different matter. The most direct approach would be to visually inspect phase portraits for various τ and m trying to identify the one that looks best. The word "best", however, might in this case be very subjective. In practice this approach for finding embedding parameters are seldom advised since we usually want to analyze a time series that originates from a rather unknown system. Then we would not know if the underlying dynamics that produced the time series had two or twenty degrees of freedom. It is easy to verify that the time required to check all possibilities that might yield a proper embedding with respect to various τ and m is very long. This being said, let it be a good motivation to discuss the average mutual information method and the false nearest neighbor method, which enable us to efficiently determine proper values of the embedding delay τ and embedding dimension m . Let us start with the mutual information method.

3.2.2 Selecting the Time Delay-

Average Mutual Information Method

A suitable embedding delay τ has to fulfill two criteria. First, τ has to be large enough so that the information we get from measuring the value of x variable at time $(i + \tau)$ is relevant and significantly different from the information we already have by knowing

the value of the measured variable at time i . Only then it will be possible to gather enough information about all other variables that influence the value of the measured variable to successfully reconstruct the whole phase space with a reasonable choice of m . Note here that generally a shorter embedding delay can always be compensated with a larger embedding dimension. This is also the reason why the original embedding theorem is formulated with respect to m , and says basically nothing about τ . Second, τ should not be larger than the typical time in which the system loses memory of its initial state. If τ would be chosen larger, the reconstructed phase space would look more or less random since it would consist of uncorrelated points. The latter condition is particularly important for chaotic systems which are intrinsically unpredictable and, hence, lose memory of the initial state as time progresses. This second demand has led to suggestions that a proper embedding delay could be estimated from the autocorrelation function where the optimal τ would be determined by the time the autocorrelation function first decreases below zero or decays to $1/\exp$. For nearly regular time series, this is a good thumb rule, whereas for chaotic time series, it might lead to spurious results since it is based solely on linear statistics and doesn't take into account nonlinear correlations.

The cure for this deficiency was introduced by Fraser and Swinney [131]. They established that delay corresponds to the first local minimum of the average mutual information function $I(\tau)$ which is defined as follows:

$$I(\tau) = \sum P(x(i), x(i+\tau)) \log_2 \left[\frac{P(x(i), x(i+\tau))}{P(x(i))P(x(i+\tau))} \right] \quad (2)$$

where $P(x(i))$, is the probability of the measure $x(i)$, $P(x(i+\tau))$ is the probability of the measure $x(i+\tau)$ and $P(x(i), x(i+\tau))$ is the joint probability of the measure of $x(i)$ and $x(i+\tau)$ [131]. The average mutual information is really a kind of generalization to the nonlinear phenomena from the correlation function in the linear phenomena. When the measures $x(i)$ and $x(i+\tau)$ are completely independent, $I(\tau)=0$. On the other hand when $x(i)$ and $x(i+\tau)$ are equal, $I(\tau)$ is maximum. Therefore plotting $I(\tau)$ versus τ makes it possible to identify the best value for the time delay, this is related to the first local minimum.

While it has often been shown that the first minimum of $I(\tau)$ really yields the optimal embedding delay, the proof of this has a more intuitive, or shall we rather say empiric, background. It is often said that at the embedding delay where $I(\tau)$ has the first local minimum, $x(i+\tau)$ adds the largest amount of information to the information we already have from knowing $x(i)$, without completely losing the correlation between them. Perhaps a more convincing evidence of this being true can be found in the very nice article by Shaw [132], who is, according to Fraser and Swinney, the idea holder of the above reasoning. However, a formal mathematical proof is lacking. Kantz and Schreiber [122] also report that in fact there is no theoretical reason why there should even exist a minimum of the mutual information. Nevertheless, this should not undermine ones trustworthiness in this particular method, since it has often proved reliable and well suited for the appointed task.

Once the time delay has been agreed upon, the embedding dimension is the next order of business. Let us now turn to establishing a proper embedding dimension m for the examined time series.

3.2.3 Selecting Embedding Dimension-

False Nearest Neighbors Method

In general, the aim of selecting an embedding dimension is to make sufficiently many observations of the system state so that the deterministic state of the system can be resolved unambiguously. It is best to remember that in the presence of observational noise and finite quantization this is not possible. Moreover, it has been shown that even with perfect observations over an arbitrary finite time interval, a correct embedding will still yield a set of states indistinguishable from the true state [133]. Most methods to estimate the embedding dimension aim to achieve unambiguity of the system state. The archetype of many of these methods is the so-called False Nearest Neighbors (FNN) technique [134-135].

The false nearest neighbor method was introduced by Kennel et al. [127] as an efficient tool for determining the minimal required embedding dimension m in order to fully resolve the complex structure of the attractor, i.e. the minimum dimension at which the reconstructed attractor can be considered completely unfolded. Again note that the embedding theorem by Takens [129] guarantees a proper embedding for all large enough m , i.e. that is also for those that are larger than the minimal required embedding dimension. In this sense, the method can be seen as an optimization

procedure yielding just the minimal required m . The method relies on the assumption that an attractor of a deterministic system folds and unfolds smoothly with no sudden irregularities in its structure. By exploiting this assumption, we must come to the conclusion that two points that are close in the reconstructed embedding space have to stay sufficiently close also during forward iteration. If this criterion is met, then under some sufficiently short forward iteration, originally proposed to equal the embedding delay, the distance between two points $X(n)$ and $X(p)$ of the reconstructed attractor, which are initially only a small distance apart, cannot grow further as we fix a threshold value for these distances in computation. However, if an n -th point has a close neighbor that doesn't fulfill this criterion, then this n -th point is marked as having a false nearest neighbor. We have to minimize the fraction of points having a false nearest neighbor by choosing a sufficiently large m . As already elucidated above, if m is chosen too small, it will be impossible to gather enough information about all other variables that influence the value of the measured variable to successfully reconstruct the whole phase space. From the geometrical point of view, this means that two points of the attractor might solely appear to be close, whereas under forward iteration, they are mapped randomly due to projection effects. The random mapping occurs because the whole attractor is projected onto a hyper plane that has a smaller dimensionality than the actual phase space and so the distances between points become distorted [136].

In order to calculate the fraction of false nearest neighbors, the following original algorithm is used.

Consider each vector $X(n) = [x(n), x(n+\tau), x(n+2\tau), \dots, x(n+(m-1)\tau)]$ in a delay coordinate embedding of the time series with delay τ and embedding dimension m . Look for its nearest neighbor $X(p)$ and $X(p) = [x(p), x(p+\tau), x(p+2\tau), \dots, x(p+(m-1)\tau)]$. The nearest neighbor is determined by finding the vector $X(p)$ in the embedding which minimizes the Euclidean distance $R_n = \|X(n) - X(p)\|$. Now consider each of these vectors under an $m+1$ dimensional embedding,

$$X'(n) = [x(n), x(n+\tau), x(n+2\tau), \dots, x(n+(m-1)\tau), x(n+m\tau)]$$

$$X'(p) = [x(p), x(p+\tau), x(p+2\tau), \dots, x(p+(m-1)\tau), x(p+m\tau)]$$

In an $m+1$ dimensional embedding, these vectors are separated by the Euclidean distance $R'_n = \|X'(n) - X'(p)\|$. The first criterion by which Kennel, et. al., identify a false nearest neighbor is if

$$\text{Criterion 1: } \left[\frac{R_n'^2 - R_n^2}{R_n^2} \right]^{1/2} = \frac{|x(n+m\tau) - x(p+m\tau)|}{R_n} > R_{tol} \quad (3)$$

R_{tol} is a unit less tolerance level for which Kennel, et. al., suggest a value of approximately 15. This criterion is meant to measure if the relative increase in the distance between two points when going from m to $m+1$ dimensions is large. 15 was suggested based upon empirical studies of several systems, although values between 10 and 40 were consistently acceptable [137]. The other criterion Kennel, et. al., suggest is

$$\text{Criterion 2: } \left[\frac{R_n'}{R_n} \right] > A_{tol} \quad (4)$$

Where A_{tol} is called absolute tolerance. This was introduced to compensate for the fact that portions of the attractor may be quite sparse. In those regions, near neighbors are not actually close to each other. Here, R_A is a measure of the size of the attractor, for which Kennel, et. al., use the standard deviation of the data. If either (3) or (4) hold, then $X(p)$ is considered a false nearest neighbor of $X(n)$. The total number of false nearest neighbors is found, and the percentage of nearest neighbors, out of all nearest neighbors, is measured. An appropriate embedding dimension is one where the percentage of false nearest neighbors identified by either method falls to zero.

The above combined criteria correctly identify a suitable embedding dimension in many cases. By now we have equipped ourselves with the knowledge that is required to successfully reconstruct the embedding space from an observed variable. This is a very important task since basically all methods of nonlinear time series analysis require this step to be accomplished successfully in order to yield meaningful results.

3.3 Time Series Analysis based on Recurrence Plots

Recurrent behaviors are typical of natural systems. In the frame work of dynamical systems, this implies the recurrence of state vectors, i.e. states with large temporal distances may be close in state space. This is a well-known property of deterministic dynamical systems and is typical for nonlinear or chaotic systems.

The formal concept of recurrences was introduced by Henri Poincare [138] in his seminal work from 1890. Even though much mathematical work was carried out in the following years, Poincare's pioneering work and his discovery of recurrence had to wait

for more than 70 years for the development of fast and efficient computers to be exploited numerically. The use of powerful computers boosted chaos theory and allowed to study new and exciting systems. Some of the tedious computations needed to use the concept of recurrence for more practical purposes could only be made with this digital tool. In 1987, Eckmann et al.[139] for the first time, introduced the method of RPs to visualize the recurrences of dynamical systems in a phase space.

3.3.1 Distance and Recurrence Matrices

Since phase spaces of more than two dimensions can only be visualized by a projection, it is hard to investigate recurrences in the state space. In the RP, any recurrence of state i with state j is pictured on a Boolean matrix expressed by

$$RP(i, j) = \Theta(\varepsilon - \|X(i) - X(j)\|), \quad i, j = 1, 2, \dots, N \quad (5)$$

Where $X(i)$ and $X(j)$ are the embedded vectors, i and j are time indices, N is the number of measured points, $\|\cdot\|$ is a norm, and ε is an arbitrary threshold radius and $\Theta(\cdot)$ is the Heaviside step function ($\Theta(X) = 0$, if $X < 0$ and $\Theta(X) = 1$ if $X \geq 0$). The RP is obtained by plotting the recurrence matrix, Eq. (5), and using different colors for its binary entries, e.g., plotting a black dot at the coordinates (i, j) , if $RP(i, j) = 1$, and a white dot, $RP(i, j) = 0$. Both axes of the RP are time axes and show rightwards and upwards (convention). Since any state is recurrent with itself, the RP matrix fulfills $RP(i, i) = 1$ by definition, the RP has always a black main diagonal line, the line of

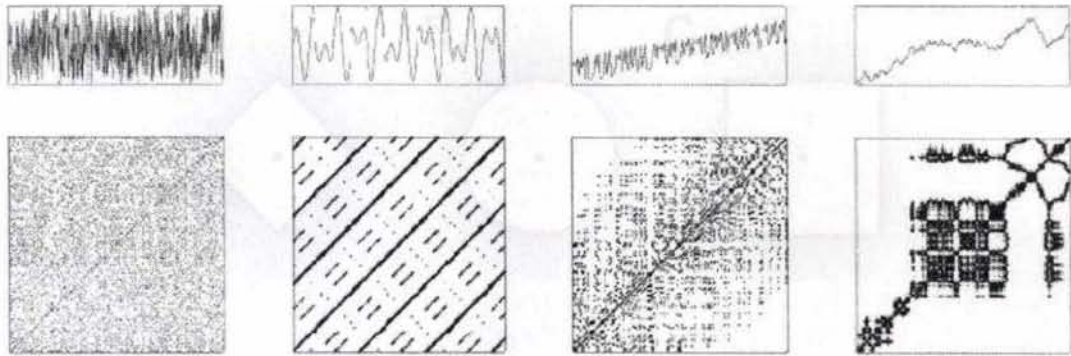


Fig. 3.1 Typical examples of recurrence plots for the neighborhood with Chebyshev radius of tolerance ϵ equal to 0.05.

A

B

C

D

Fig. 3.1 Typical examples of recurrence plots (top row: time series (plotted over time); bottom row: corresponding recurrence plots). From left to right: (A) uncorrelated stochastic data (white noise), (B) harmonic oscillation with two frequencies, (C) chaotic data with linear trend (logistic map) and (D) data from an auto-regressive process.

Identity (LOI). Furthermore, the RP is symmetric by definition with respect to the main diagonal, i.e. $RP(i, j) = RP(j, i)$. Figure 3.1 shows typical examples of RPs.

In order to compute an RP, an appropriate norm has to be chosen. As implied by its name, the norm function geometrically defines the size (and shape) of the neighborhood surrounding each reference point. The most frequently used norms are the L_1 -norm, the L_2 -norm (Euclidean norm) and the L_∞ -norm (Maximum or Supernorm norm). The neighborhoods of these norms have different shapes (Figure 3.2). Considering a fixed ϵ , the L_∞ -norm finds the most, the L_1 -norm the least and the L_2 -norm an intermediate amount of neighbors [140]. Since a vector must have at least two points, each norm is unique if and only if $m > 1$, else all norms are exactly equivalent for $m = 1$. Computed distance values are distributed within a distance matrix, DM of size

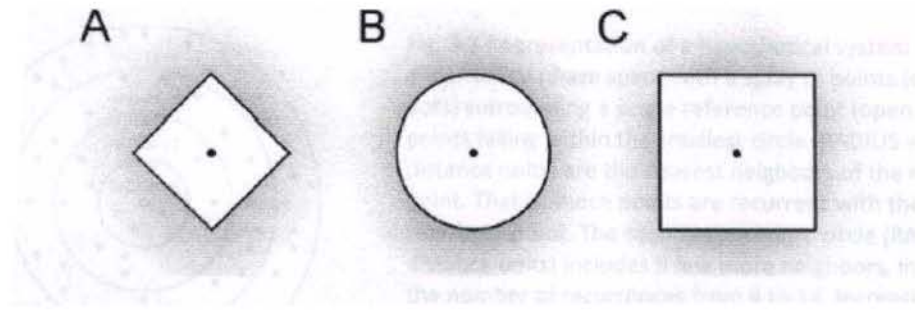


Fig. 3.2 Three commonly used norms for the neighborhood with the same radius around a point (black dot) exemplarily shown for the two-dimensional phase space: (A) L_1 -norm, (B) L_2 -norm and (C) L_∞ -norm.

$W \times W$, where $W = N - m + 1$. The DM , therefore, has W^2 elements with a long central diagonal of W distances all equal to zero. This value of W is valid for a delay of 1. A more general value for W is then $W = N - (m-1)\tau$. Now the Recurrence matrix RM is derived from DM by setting the threshold radius, ε . The Heaviside function assigns values of 0 or 1 to array elements in the RM . Only those distances in $RM(i, j)$ equal to or less than ε are defined as recurrent points at coordinates (i, j) [Appendix 1]

3.3.2 Threshold Radius

A crucial parameter of an RP is the threshold radius, ε . Therefore, special attention has to be required for its choice. If ε is chosen too small, there may be almost no recurrence points and we cannot learn anything about the recurrence structure of the underlying system. On the other hand, if ε is chosen too large, almost every point is a neighbor of every other point, which leads to a lot of artifacts. A too large ε includes also points into the neighborhood which are simple consecutive points on the

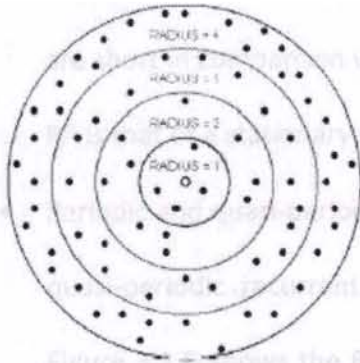


Fig. 3.3 Representation of a hypothetical system in higher-dimensional phase space with a splay of points (closed dots) surrounding a single reference point (open dot). The points falling within the smallest circle (RADIUS = 1 distance units) are the nearest neighbors of the reference point. That is, those points are recurrent with the reference point. The second concentric circle (RADIUS = 2 distance units) includes a few more neighbors, increasing the number of recurrences from 4 to 14. Increasing the radius further (RADIUS = 3 or 4 distance units) becomes too inclusive, capturing an additional 20 or 60 distant points as nearest neighbors when, in fact, they are not.

trajectory. This effect is called tangential motion and causes thicker and longer diagonal structures in the RP as they actually are. Hence, we have to find a compromise for the value of ϵ . The “shotgun plot” of Figure 3.3 provides a conceptual framework for understanding why an increasing threshold radius captures more and more recurrent points in phase space. For simplicity, in this thesis the threshold radius will be referred to as RADIUS. Proper procedures for selecting the optimal RADIUS parameter is described under section 3.3.5

3.3.3 Structures in Recurrence Plots

As already mentioned, the initial purpose of RPs was to visualize trajectories in phase space, which is especially advantageous in the case of high dimensional systems. RPs yield important insights into the time evolution of these trajectories, because typical patterns in RPs are linked to a specific behavior of the system. Large scale patterns in RPs, designated in [139] as typology, can be classified in homogeneous, periodic, drift and disrupted ones [139,140]:

- Homogeneous RPs are typical of stationary systems in which the relaxation times are short in comparison with the time spanned by the RP. An example of such an RP is that of a stationary random time series (Figure 3.1 A).
- Periodic and quasi-periodic systems have RPs with diagonal oriented, periodic or quasi-periodic recurrent structures (diagonal lines, checkerboard structures). Figure 3.1.B shows the RP of a periodic system with two harmonic frequencies and with a frequency ratio of four (two and four short lines lie between the continuous diagonal lines). Irrational frequency ratios cause more complex quasi-periodic recurrent structures (the distances between the diagonal lines are different). However, even for oscillating systems whose oscillations are not easily recognizable, RPs can be useful
- A drift is caused by systems with slowly varying parameters, i.e. non-stationary systems. The RP pales away from the LOI (Figure 3.1. C).
- Abrupt changes in the dynamics as well as extreme events cause white areas or bands in the RP (Figure 3.1.D). RPs allow finding and assessing extreme and rare events easily by using the frequency of their recurrences.

A closer inspection of the RPs reveals also small-scale structures, the texture [139], which can be typically classified in single dots, diagonal lines as well as vertical and horizontal lines (the combination of vertical and horizontal lines obviously forms rectangular clusters of recurrence points); in addition, even bowed lines may occur [139,140]. Table 3.2 tabulates typical patterns in RPs and their meanings

- Single, isolated recurrence points can occur if states are rare, if they persist only for a very short time, or fluctuate strongly.
- A diagonal line $R(i+k, j+k) \equiv 1_{k=0}^{l-1}$ (where l is the length of the diagonal line) occurs when a segment of the trajectory runs almost in parallel to another segment (i.e. through an ε -tube around the other segment, Figure 3.4) for l time units. The length of this diagonal line is determined by the duration of such similar local evolution of the trajectory segments. The direction of these diagonal structures is parallel to the LOI (slope one, angle $\pi/4$). They represent trajectories which evolve through the same ε -tube for a certain time.
- A vertical (horizontal) line $R(i, j+k) \equiv 1_{k=0}^{v-1}$ (with v the length of the vertical line) marks a time interval in which a state does not change or changes very slowly. Hence, the state is trapped for some time. This is a typical behavior of laminar states (intermittency) [141].

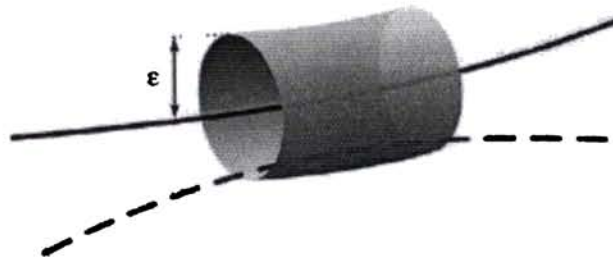


Fig. 3. 4. A diagonal line in a RP corresponds with a section of a trajectory (dashed) which stays within an ε -tube around another section (solid).

- Bowed lines are lines with a non-constant slope. The shape of a bowed line depends on the local time relationship between the corresponding close trajectory segments.

Table 3.2 Typical patterns in RPs and their meanings

Pattern	Meaning
1 Homogeneity	The process is stationary
2 Fading to the upper left and lower right corners	Non-stationary data; the process contains a trend or a drift
3 Disruptions (white bands)	Non-stationary data; some states are rare or far from the normal; transitions may have occurred.
4 Periodic/quasi-periodic patterns	Cyclicities in the process; the time distance between periodic patterns (e.g. lines) corresponds to the period; different distances between long diagonal lines reveal quasi-periodic processes
5 Single isolated points	Strong fluctuation in the process; if only single isolated points occur, the process may be an uncorrelated random or even anti-correlated process
6 Diagonal lines (parallel to the LOI)	The evolution of states is similar at different epochs; the process could be deterministic; if these diagonal lines occur beside single isolated points, the process could be chaotic (if these diagonal lines are periodic, unstable periodic orbits can be observed)
7 Diagonal lines (orthogonal to the LOI)	The evolution of states is similar at different times but with reverse time; sometimes this is an indication for an insufficient embedding
8 Vertical and horizontal lines/clusters	Some states do not change or change slowly for some time; indication for laminar states
9 Long bowed line structures	The evolution of states is similar at different epochs but with different velocity; the dynamics of the system could be changing

The visual interpretation of RPs requires some experience. RPs of paradigmatic systems provide an instructive introduction into characteristic typology and texture (e.g. Figure 3.1). However, a quantification of the obtained structures is necessary for a more objective investigation of the considered system.

3.3.4 Measures of complexity - Recurrence Quantification Analysis

Instead of trusting one's eye to "see" recurrence patterns, specific rules had to be devised whereby certain recurrence features could be automatically extracted from RPs. In so doing, problems relating to individual biases of multiple observers and subjective interpretations of RPs were categorically precluded.

With an objective to go beyond the visual impression yielded by RPs, several measures of complexity which quantify the small-scale structures in RPs have been proposed in [141-143] and are known as RQA. These measures are based on the recurrence point density and the diagonal and vertical line structures of the RP. A computation of these measures in small windows or otherwise called epochs (sub-matrices) of the RP moving along the LOI yields the time dependent behavior of these variables. Some studies based on RQA measures show that they are able to identify bifurcation points, especially chaos-order transitions [144]. The vertical structures in the RP are related to intermittency and laminar states. Those measures quantifying the vertical structures enable also to detect chaos-chaos transitions [141].

As the RP is symmetrical across the central diagonal, all quantitative feature extractions take place within the upper triangle in the RP [145], excluding the long diagonal (which provides no unique information) and lower triangle (which provides only redundant information). We can derive eight statistical values from a RP using RQA. The first value is percent recurrence(%REC), quantifies the percentage of recurrent points falling within the specified radius. For a given window size W ,

$$\text{Percent recurrence} = \frac{\text{Number of recurrent points in triangle} * 100}{(W(W - 1) / 2)} \quad (6)$$

Here W refers to the recurrence window size after accounting for embedding and delay; ie. $W = [(N_2 - N_1 + 1) - (m - 1)\tau]$ where N_1 and N_2 are the first and last points of the window considered.

The second variable is percent determinism (%DET) and measures the percentage of recurrent points that are contained in lines parallel to the main diagonal of the RP, which are known as deterministic lines. A deterministic line is defined if it contains a predefined minimum number of recurrence points. It represents a measure of predictability of the system.

$$\text{Percent determinism} = \frac{\text{Number of points in diagonal lines} * 100}{\text{Number of recurrence points}} \quad (7)$$

The third recurrence variable is Linemax (LMAX), which is simply the length of the longest diagonal line segment in the plot, excluding the main diagonal LOI (where $i = j$). This is a very important recurrence variable because it inversely scales with the most

positive Lyapunov exponent [139,144]. Positive Lyapunov exponents gauge the rate at which trajectories diverge, and are the hallmark for dynamic chaos.

$$\textit{Linemax} = \textit{length of longest diagonal line in recurrence plot} \quad (8)$$

The fourth variable value is called entropy (ENT) and it refers to the Shannon entropy of the distribution probability of the diagonal lines length. ENT is a measure of signal complexity and is calibrated in units of bits/bin and is calculated by binning the deterministic lines according to their length. Individual histogram bin probabilities (P_{bin}) are computed for each non-zero bin and then summed according to Shannon's equation.

$$\textit{Entropy} = -\sum (P_{bin}) \log_2(P_{bin}) \quad (9)$$

The fifth statistical value is the Trend (TND) which is used to detect non-stationarity in the data. The trend essentially measures how quickly the RP pales away from the main diagonal and can be utilized as a measure of stationarity. If recurrent points are homogeneously distributed across the RP, TND values will hover near zero units. If recurrent points are heterogeneously distributed across the RP, TND values will deviate from zero units. TND is computed as the slope of the least squares regression of percent local recurrence as a function of the orthogonal displacement from the central diagonal. Multiplying by 1000 increases the gain of the TND variable.

$$\textit{Trend} = 1000(\textit{slope of percent local recurrence vs. displacement}) \quad (10)$$

For the detection of chaos-chaos transitions, Marwan et al. [141] introduced other two additional RQA variables, the Percent Laminarity(%LAM) and Trapping time(TT), in which attention is focused on vertical line structures and black patches. %LAM is analogous to %DET except that it measures the percentage of recurrent points comprising vertical line structures rather than diagonal line structures. The line parameter still governs the minimum length of vertical lines to be included.

$$\text{Percent Laminarity} = \frac{\text{Number of points in vertical lines} * 100}{\text{Number of recurrent points}} \quad (11)$$

TT on the other hand is the average length of vertical line structures. It represents the average time in which the system is “trapped” in a specific state.

$$\text{Trapping time} = \text{average length of vertical lines} \geq \text{parameter line} \quad (12)$$

The eighth recurrence variable is VMAX, which is simply the length of the longest vertical line segment in the plot. This variable is analogous to the standard measure LMAX

$$V_{max} = \text{length of longest vertical line in recurrence plot} \quad (13)$$

3.3.5 Selection of the Threshold Radius

There are three guidelines for selecting the proper radius (in order of preference):

- (i) RADIUS must fall with the linear scaling region of the double logarithmic plot;
- (ii) %REC must be kept low (e.g., 0.1 to 2.0%); and

(iii) RADIUS may or may not coincide with the first minimum hitch in %DET.

Weighing all three factors together, a radius of 15% was selected for an example data (vertical dashed lines in Figure 3.5), which fits all three criteria. Because there are mathematical scaling rules linking $\log(\%REC)$ with $\log(RADIUS)$, as will be discussed below, the first guideline for RADIUS selection is preferred. In contrast, since there are no known rules describing the hitch region in %DET, this latter method must be applied with caution. Nevertheless, the choice of ϵ depends strongly on the considered system under study.

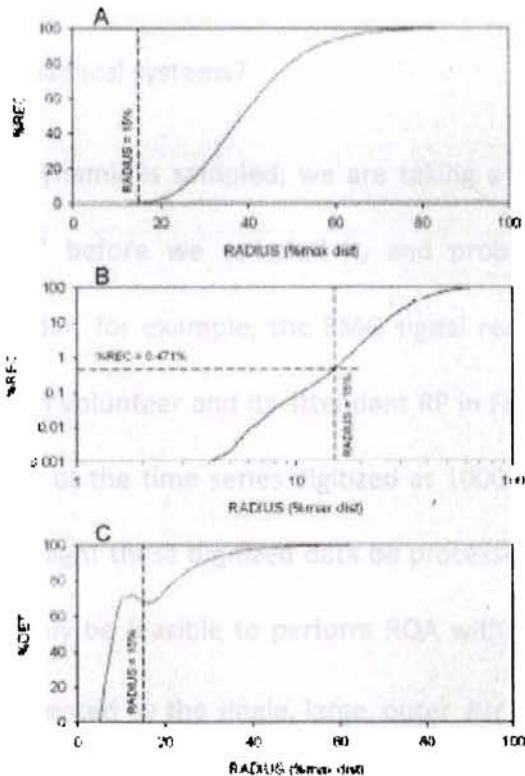


Fig. 3.5 Methods for selecting the proper radius parameter for recurrence analysis of a sample data

(A) With step increases in RADIUS, the density of recurrence points (%REC) increases along a sigmoid curve.

(B) Double-logarithmic plot of %REC as a function of RADIUS defines a linear scaling region from RADIUS = 8% to 15%. RADIUS is selected at 15% where %REC is 0.471% (sparse recurrence matrix).

(C) Linear plot of %DET as a function of RADIUS showing a short plateau and small trough near RADIUS = 15% which may or may not be coincidental.

3.3.6 Episodic Recurrences

So far we have demonstrated that time series data can be embedded into higher dimensional space by the method of time delays (Takens, 1981). Distances between all possible vectors are computed and registered in a distance matrix, specific distance values being based on the selected norm parameter. A recurrence matrix (RM) is derived from the distance matrix (DM) by selecting an inclusive radius parameter such that only a small percentage of points with small distances are counted as recurrent (yielding a sparse RM). The RP, of course, is just the graphical representations of RM elements at or below the radius threshold. Eight features (recurrence variables) are extracted from the RP within each window (W) of observation on the time series. The question before us now is how can these recurrence variables be useful in the diagnosis of dynamical systems?

Any dynamic is sampled; we are taking a “slice of life,” as it were. The dynamic was “alive” before we sampled it, and probably remained “alive” after our sampling. Consider, for example, the EMG signal recorded from the biceps muscle of a normal human volunteer and its attendant RP in Figure 3.6 [146]. The focus is on the first 1972 points of the time series digitized at 1000 Hz (displayed from 37 ms to 1828 ms). But how might these digitized data be processed in terms of recurrence analysis? It would certainly be feasible to perform RQA within the entire window ($W_{large} = 1972$ points) as represented by the single, large, outer RM square. On the other hand, the data can be windowed into four smaller segments ($W_{small} = 1024$ points) as represented by the four

smaller and overlapping RM squares. In the latter case the window offset of 256 points means the sliding window jogs over 256 points (256 ms) between windows. Two effects are at play here. First, larger windows focus on global dynamics(longer time frame) whereas smaller windows focus on local dynamics (shorter time frame). Second, larger window offsets yield lower time resolution RQA variables, whereas smaller window offsets yield higher time-resolution variables. Remember, eight RQA variables are computed (extracted) from each RM (or RP).

By implementing a sliding window design(termed epochs), each of those variables is computed multiple times, creating seven new derivative dynamical systems expressed in terms of %REC, %DET, LMAX, ENT, TND, %LAM, TT and VMAX. Alignment of those variables (outputs) with the original time series (input) (adjusting for the embedding dimension, m) might reveal details not obvious in the 1- dimensional input data. This EMG example illustrates the power of sliding recurrence windows.

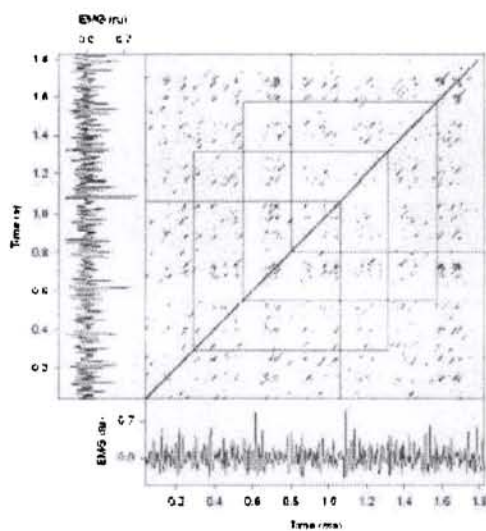


Fig. 3.6 Windowed recurrence analysis of EMG signal. The large outer square displays the large scale recurrence plot ($W = 1792 = N$ points). The four small inner squares (epochs) block off the small scale recurrence plots ($W = 1024 < N$) with an offset of 256 points between windows.

3.4 Summary

Recurrence is a fundamental property of dynamical systems, which can be exploited to characterize the system's behavior in phase space. In this chapter a comprehensive overview of nonlinear time series analysis methodology, covering recurrence based methods is provided. In the following chapter we look at the research methodology adopted for this thesis work.

Chapter 4 - Research Methodology

This chapter presents the research methodology adopted in this thesis. It is based on nonlinear dynamics concepts and time series analysis through state space embedding and recurrence plots. It therefore makes use of the knowledge gained in previous chapters for sensor signal analysis.

4.1 Procedure

The problem in hand applies RQA based methodology for data analysis and feature extraction (Figure 4.1). The recorded time series data (sensor signals) representing value fluctuations in one or more state variables is transformed into a sequence of points in a higher-dimensional space by applying the Taken's time-lag embedding theorem. This process is called attractor reconstruction. A symmetric matrix called distance matrix is then obtained from the points on the trajectory of this attractor. By setting a threshold radius and using a Heaviside function, this distance matrix is transformed into a recurrence matrix. The RP is obtained by plotting this recurrence matrix which shows all the recurrent points as dark spots. Only those distances in the recurrence matrix equal

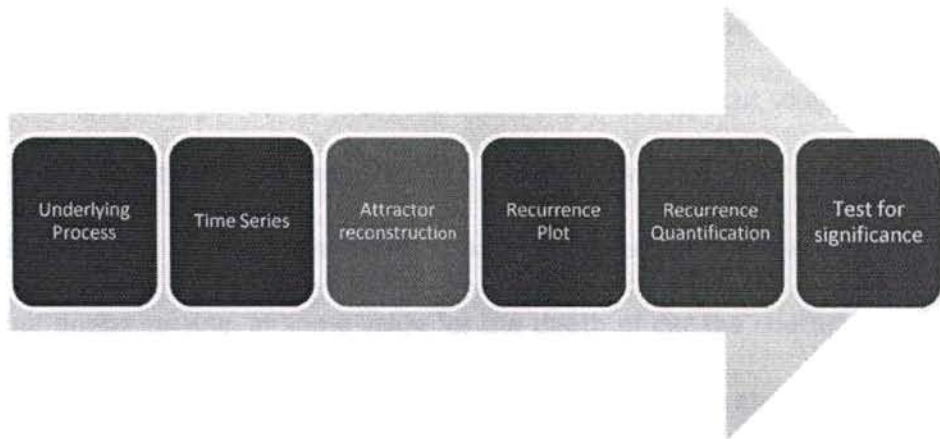


Fig. 4.1 Research Methodology

to or less than the threshold radius are defined as recurrent points. In order to quantify the differently appearing recurrence plots based on the small-scale structures therein, an RQA is carried out. The RQA outputs values of a number of measures of complexity called RQA variables, all of which are then subjected to statistical tests for significance; Mann Whitney U-test . The significant ones among them are taken as characteristics of the dynamics of the processes under study. The study then utilizes these identified significant features for detecting tool wear and chatter.

The work consists of two different sets of experiments in a lathe; set-1 and set-2. The experiment, set-1, study the influence of tool wear on the RQA variables whereas the set-2 is carried out to identify the sensitive RQA variables to machine tool chatter followed by its validation in actual cutting. To obtain the bounds of the spectrum of the significant RQA variable values, in set-1, a fresh tool and a worn tool are used for cutting. The first part of the set-2 experiments uses a stepped shaft in order to create

chatter at a known location. And the second part uses a conical section having a uniform taper along the axis. This particular design causes the depth of cut to increase smoothly and at a constant rate when the other two cutting parameters; the rpm and feed rate, are held constant. Since all other cutting parameters except the depth of cut remains the same during cutting, at some value for the depth of cut the chatter is expected to onset. The second effort, therefore, is to locate this point by the above methodology.

The various components involved in the analysis and their implementation etc. like NTSA, RP and RQA have been discussed in the previous chapters. In the following section the non-parametric U test is discussed for completion of the methodology.

4.2 Mann-Whitney U test

In statistics, the Mann-Whitney U test (also called the Mann-Whitney-Wilcoxon (MWW), Wilcoxon rank-sum test, or Wilcoxon-Mann-Whitney test) is a non-parametric test for assessing whether two samples of observations come from the same distribution. The null hypothesis is that the two samples are drawn from a single population, and therefore that their probability distributions are equal. It requires the two samples to be independent, and the observations to be ordinal or continuous measurements, i.e. one can at least say, of any two observations, which is the greater. More generally, the Wilcoxon-Mann-Whitney two-sample test may be thought of as testing the null hypothesis that the probability of an observation from one population exceeding an observation from the second population is equal to 0.5.

It is one of the best-known non-parametric significance tests. It was proposed initially by Wilcoxon for equal sample sizes, and extended to arbitrary sample sizes and in other ways by Mann and Whitney [147]. MWW is virtually identical to performing an ordinary parametric two-sample U test on the data after ranking over the combined samples. The method is illustrated in Appendix 2.

Chapter 5 - Experimental setup and Data Acquisitions

In this chapter, the experimental setup, the data acquisition systems and the different work pieces that are used in the experiments are discussed.

5.1 Description of the Machine Tool

All experiments are conducted in a 3 phase, 3.7 kW, 1400-rpm PSG heavy-duty lathe using CNMG 120408 PM carbide inserts with standard tool holder. The work pieces are circular in cross section and are made of mild steel. It is held firmly between centers; a four jaw chuck and a revolving centre. The cutting factors; speed (560 rpm) and feed per revolution (0.06 mm) are maintained constant for all sets of experiments while the depth of cut is varied as designed in the particular set. During cutting, the tool overhang is set to 12 mm. No coolants or lubricants were used during the operation.

5.2 Details of the Test Specimen

Three work pieces of different geometries are used in the experiments. The Set-1 experiment uses a rod of uniform cross section of diameter 30 mm as shown in Figure 5.1. The Set-2 experiments consist of two parts; Part-1 and Part-2. The experiment

Part-1 uses a stepped shaft whereas Part-2 uses a conical shaped rod as shown in Figure 5.2.

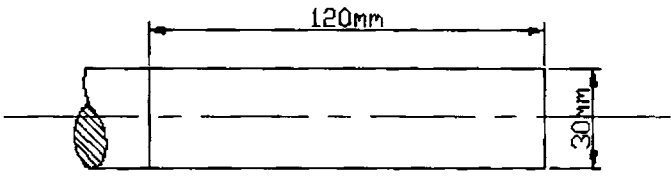
Work piece geometry	Cutting Factors
 <p>The diagram shows a cylindrical workpiece with a total length of 120mm and a diameter of 30mm. A hatched section at the left end represents the cutting tool.</p>	<p>Speed – 560 rpm Feed – 0.06 mm /rev. Depth of cut – 0.2 mm</p>

Fig. 5.1 Test Configuration for Experiment Set-1

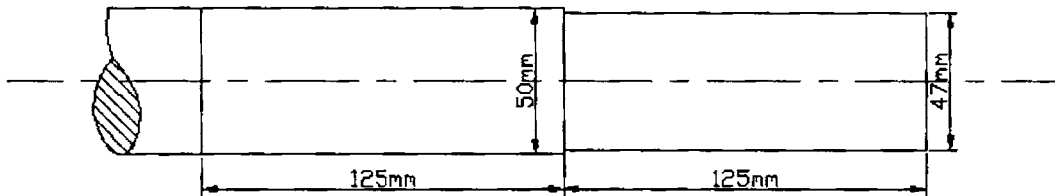
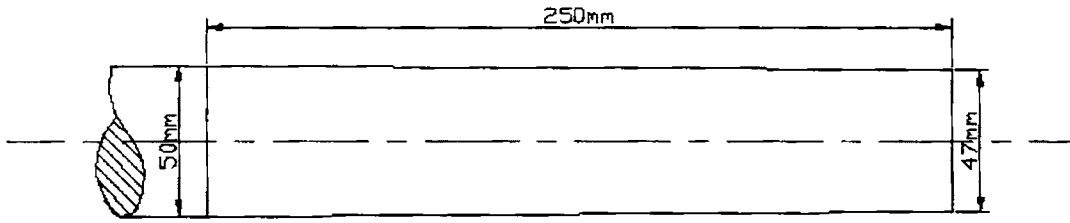
 <p>The diagram shows a stepped shaft with a total length of 250mm. The first 125mm section has a diameter of 50mm, and the second 125mm section has a diameter of 47mm. A hatched section at the left end represents the cutting tool.</p>	<p>Speed – 560 rpm , Feed – 0.06 mm/rev. Depth of cut – 0.2 mm for the first 125 mm length and 1.7 mm thereafter</p>
 <p>The diagram shows a conical rod with a total length of 250mm. The diameter starts at 50mm on the left and tapers to 47mm on the right. A hatched section at the left end represents the cutting tool.</p>	<p>Conical section, Speed – 560 rpm, Feed – 0.06 mm/rev. Depth of cut – gradually increase from 0.2 mm at the 47 mm dia to 1.7 mm at the 50 mm dia.</p>

Fig. 5.2 Test configuration for Experiment Set-2

5.3 Specifications of Tool Insert

The cutting tool used in all the experiments is CNMG 120408 PM carbide inserts with standard tool holder. In Experiment Set-1 two different quality inserts having different amount of flank wear are used. Here a fresh tool is characterized by flank wear=0 mm and a worn tool has a flank wear =0.3 mm. The flank wear is measured using TESA VISIO-300, a non contact measuring instrument utilizing machine vision technology.

5.4 Description of the Data Acquisition System-Sensors

During the experiments two sensors are used. One is a lathe drive motor current sensor and the other is an accelerometer for picking tool vibrations. When used together, the sensor measurements are made simultaneously.

5.4.1 Current Sensor

The data acquisition system for drive motor current uses a 3 phase line current sensor to measure the current drawn by the lathe drive motor. The sensor consists of three current transformers (CT) having an output range of ± 5 volts. The analog voltage signal from the output of the CT is sent to DAC NI PCI 6221 through NI SHC68-68-EPM and SCB 68 for converting it to the digital domain. The sampling rate is fixed at 500Hz which guaranteed that the whole frequency domain contained in the signal is covered. The digitized data is recorded in the PC hard drive using NI LabVIEW. A flow diagram for the sensor setup is given in Figure 5.3

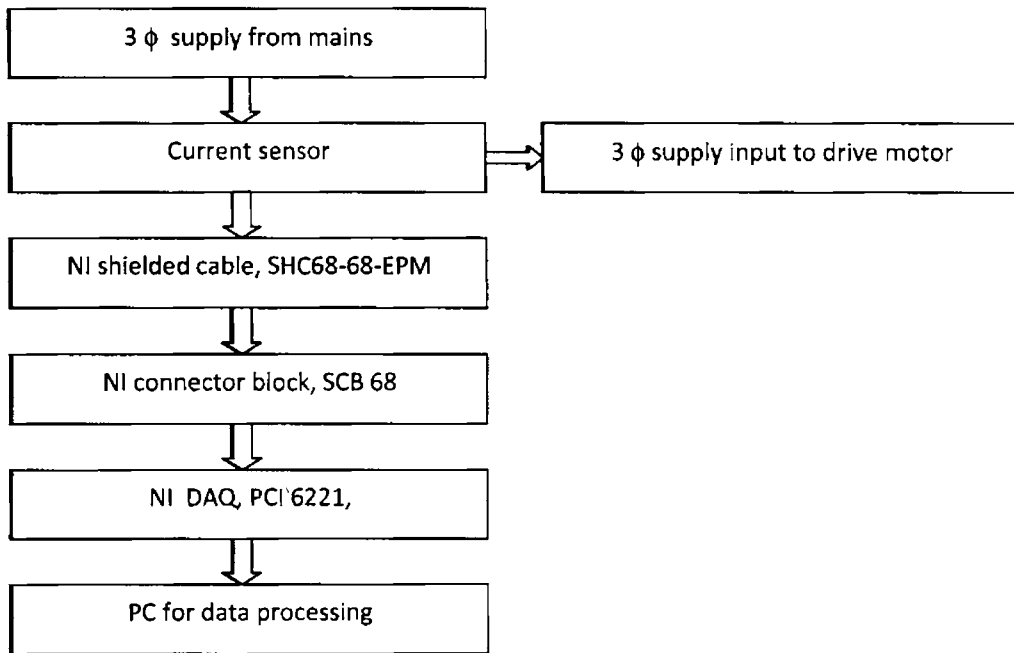


Fig. 5.3 Data acquisition flow diagram for the current sensor.

5.4.2 Vibration Sensor

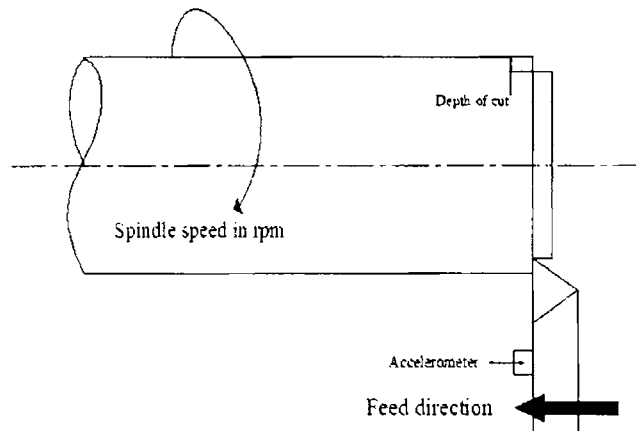


Fig. 5.4 Turning operation showing positioning of accelerometer on tool holder

An ADXL-150 accelerometer sensor, is used to pick up the vibration of the cutting tool. It is placed on the tool holder near its tail end to measure vibration in the feed direction. The resulting output voltage signal, due to vibration, is amplified and passed through a low pass filter having a cut-off frequency of 1 kHz. Here the sampling rate is fixed at 10 kHz. The data acquisition system for vibration signals used a different channel of the same DAC NI PCI 6221 and similarly other peripherals along with NI LabVIEW. Figure 4.2 shows the data acquisition flow diagram for the accelerometer.

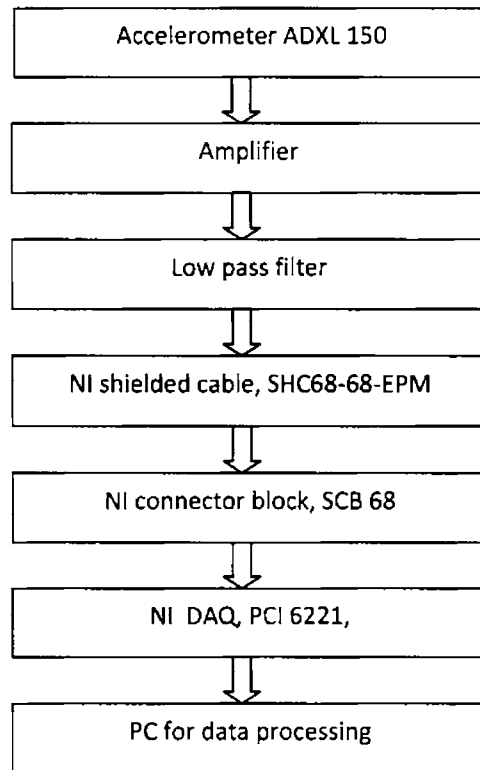


Fig. 5.5 Data acquisition flow diagram for the current sensor.

5.5 NI DAQ components

- DAC NI PCI 6221

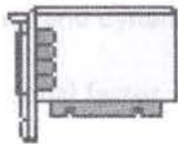
Data acquisition card with two 16-bit analog outputs (833 kS/s); 24 digital I/O; 32-bit counters

- SHC68-68-EPM

This cable is designed to work with NI PCI 6221. It includes separate digital and analog sections, individually shielded twisted pairs for analog inputs, individually shielded analog outputs, and twisted pairs for critical digital I/O.

- SCB 68

Noise rejecting, shielded I/O connector block for NI PCI 6221 with 68-Pin Connectors



NI PCI-6221



Cable



Connector Block

Fig. 5.6 NI DAQ components

5.6 ADXL 150 Accelerometer

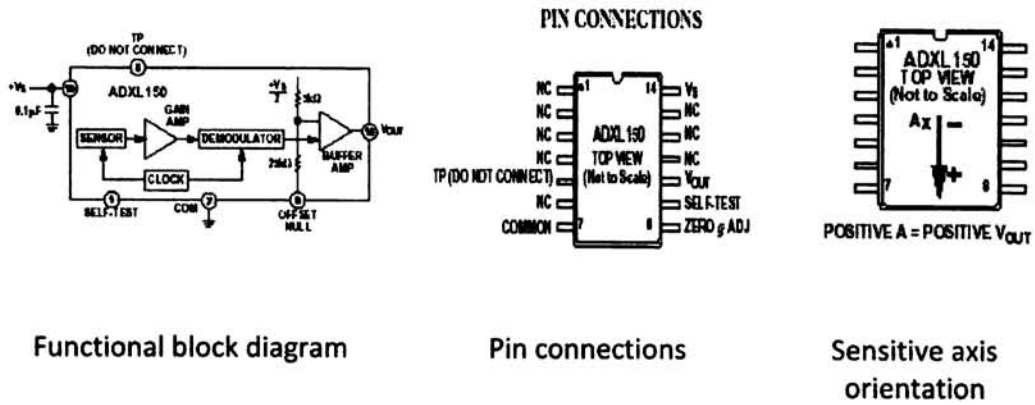
In order to detect vibrations of the lathe cutting tool a transducer is required and it is for converting the mechanical vibrations to proportional electrical signals. This is the reason an acceleration sensitive transducers, called accelerometers is opted here An

accelerometer is an electromechanical transducer which produces at its output terminals, a voltage or charge that is proportional to the acceleration to which it is subjected. The piezoelectric elements (similar to small crystals) within the accelerometer have the property of producing an electrical charge which is directly proportional to the strain and hence to the applied force when loaded either in tension, compression or shear. For frequencies lying well under the resonant frequency of the assembly, the acceleration of the masses will be the same as the acceleration of the base, and the output signal level will be proportional to the acceleration to which the accelerometer is subjected.

Reasons for the transfer of preference towards accelerometers are that they are generally much smaller in terms of relative mass than velocity pickups and that their frequency and dynamic ranges are significantly wider, even after integration to velocity. An additional factor which underlines the benefits of accelerometers is the fact that an accelerometer signal can be easily and validly integrated electronically to obtain velocity and displacement. Moreover it is very cheap.

The ADXL 150 is a third generation $\pm 50g$ surface micro accelerometer (Figure 5.7). It offers lower noise, wider dynamic range, reduced power consumption and improved zero g bias drift. It is a single axis accelerometer with signal conditioning on a single monolithic IC. Power consumption is modest at 1.8mA per axis. The ADXL 150 is available in a hermetic 14-lead surface mount cerpac package specified over the 0° to $+70^\circ$ C commercial and -400° C to $+85^\circ$ C industrial temperature ranges. Generally used in

Vibration measurement, Shock detection, Machine condition monitoring, Fleet monitoring and Event recording



Functional block diagram
Pin connections
Sensitive axis orientation

Fig. 5.7 ADXL 150 accelerometer details

5.7 Block Schematic of Current sensor

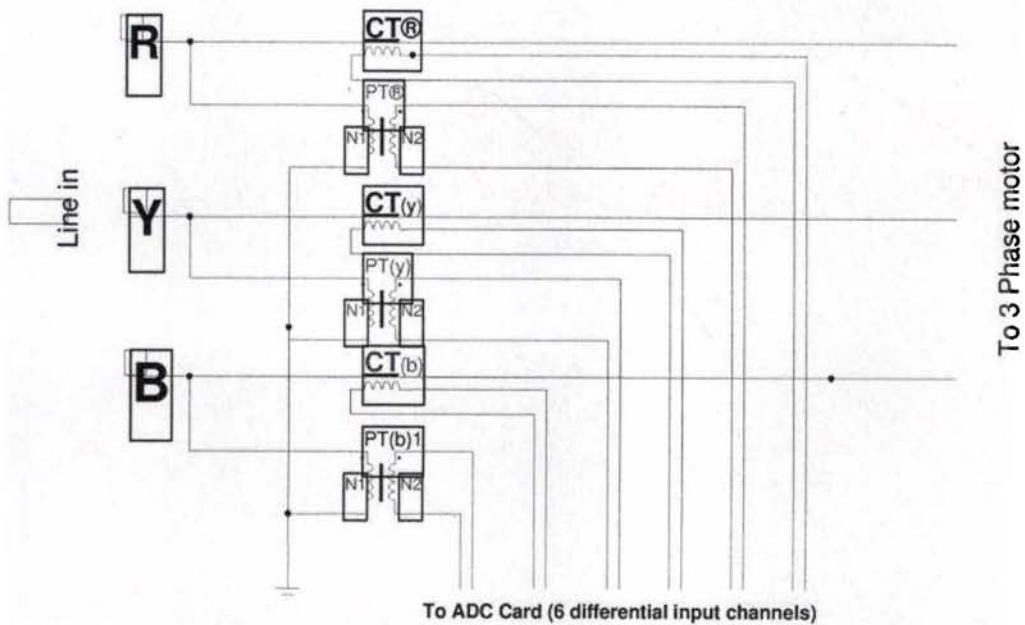


Fig. 5.8 Block schematic of the voltage and current measurement setup

The voltage and currents in each phase is measured by using three power transformers and current transformers. They are laid as shown in Figure 5.8 The output of the transformers have an output range of ± 5 volts. The signals are taken out through shielded cables.

5.8 Summary

All the experiments are conducted on a conventional lathe with standard tool inserts and tool holder. Two sensors; one accelerometer and one current sensor are used during the experiments and three work pieces of different geometries are tested. In the next chapter the experiments and the results are discussed.

Chapter 6 - Experiments and Results

In this chapter the different experiments conducted are described and their results are presented. The chapter is organized into two sections. Description of Experiment Set-1 and their outcome are given in the first section and Experiment Set-2 is given under the second section of the chapter

EXPERIMENT SET 1 - TOOL WEAR

In this experimental study, the powerful method of RQA is utilized to study and characterize the recorded experimental sensor signals; in order to discriminate the signals generated during the process with cutting tools having different degrees of flank wear on them. The study also explored the effectiveness of applying the system input signal, drive motor current in relation to a system output signal, the tool vibration for the analysis.

6.1.1 Experiments and Data Acquisition

Experiments are conducted on the 3 phase, 3.7 kW, 1400-rpm PSG heavy-duty lathe using CNMG 120408 PM carbide inserts with standard tool holder. The work pieces are made of 30 mm diameter and 120 mm long mild steel rods (Figure 5.1). The machining job in the experiment involves reducing the diameter of the work piece to 29.6 mm in a single pass of the tool from the original 30 mm. The cutting factors; speed (560 rpm), feed per revolution (0.06 mm) and depth of cut (0.2 mm) are maintained constant during the experiments. For the experiment, a fresh tool is characterized by flank wear=0 mm and a worn tool has a flank wear =0.3 mm.

Two arrays of experiments, one with the fresh tool and the other with the worn tool, containing 7 trials in each array are conducted. Using the current and vibration sensors, continuous data is recorded for a cut of 10 sec duration through separate channels available in the DAQ, during every trial of the experiments, at the designed sampling rates. Thus, a total of 14 numbers of experiments are conducted and simultaneous recordings of sensor signals representing time history of lathe drive motor current as well as tool vibrations during cutting are done, resulting in 14 data sets in each of the two arrays.

From each of the dataset so recorded 1000 data points representing a 2 sec duration of cut for the current sensor signal and, similarly, 1000 data points representing a 0.1 sec duration for the vibration sensor signal, are randomly selected and analyzed.

6.1.2 Data Analysis

6.1.2.1 Recurrence Quantification Analysis

As already detailed, the most basic step in this procedure is to construct a proper embedding space from the data set representing time series. For this purpose, we determine the proper embedding delay and embedding dimension, following the AMI and FNN methods.

The values for τ and m for the fresh tool and worn tool have been calculated and are shown in Table 6.1. It may be noted that, the time lag values for both the sensor signals for the two types of tools matches whereas their embedding dimensions differs, shows a higher value for the worn tool. Figures 6.1 and 6.2 shows sample plots for the worn tool using current sensor data.

Since the work is aimed at monitoring of tool wear that takes place progressively as cutting takes place, phase space reconstruction using two different sets of values is avoided here. Instead, they are chosen from the representative values of the worn tool which demands higher embedding dimension. Table 6.2 shows the values used in subsequent analysis.

Table 6. 1. Phase space reconstruction parameters obtained by AMI and FNN

	Time delay, τ		Embedding dimension, m	
	Current signal	Vibration Signal	Current signal	Vibration Signal
Fresh Tool	3	6	3	5
Worn Tool	3	6	5	7

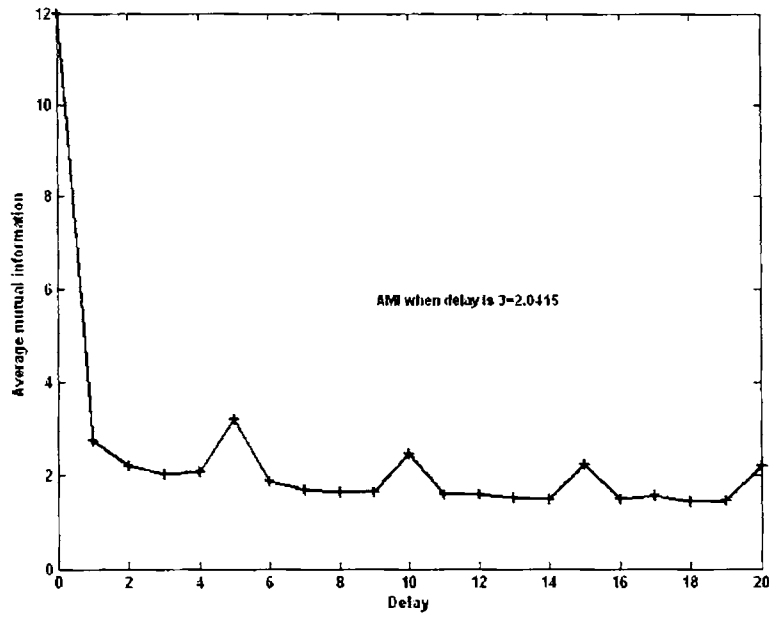


Fig. 6.1 Delay Vs. AMI plot for worn tool – Current sensor data

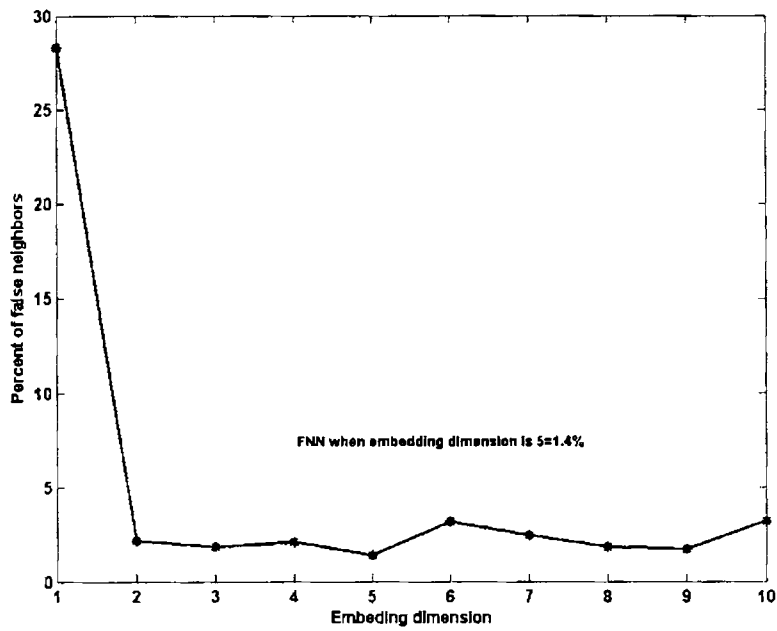


Fig. 6.2 Embedding dimension Vs. FNN plot for worn tool – Current sensor data

Table 6. 2. Phase space reconstruction parameters actually used in the analysis.

	Time lag, τ		Embedding dimension, m	
	Current signal	Vibration Signal	Current signal	Vibration Signal
Fresh Tool	3	6	5	7
Worn Tool	3	6	5	7

The next stage in the procedure is Recurrence Plot construction. Before doing that it is necessary to select the type of norm to use in distance calculations for DM from which we derive RM . In the present analysis recurrence plots are constructed applying L_2 norm in distance calculations. The next crucial parameter in RP construction is the threshold radius, ϵ . It is chosen by analyzing the measure of recurrence point density as percentage of maximum distance [145] (Table 6.3). Again, as followed and due to reasons assumed in phase reconstruction, we use the threshold ϵ values obtained for the worn tool as representative values for RQA estimation as shown in Table 6.4.

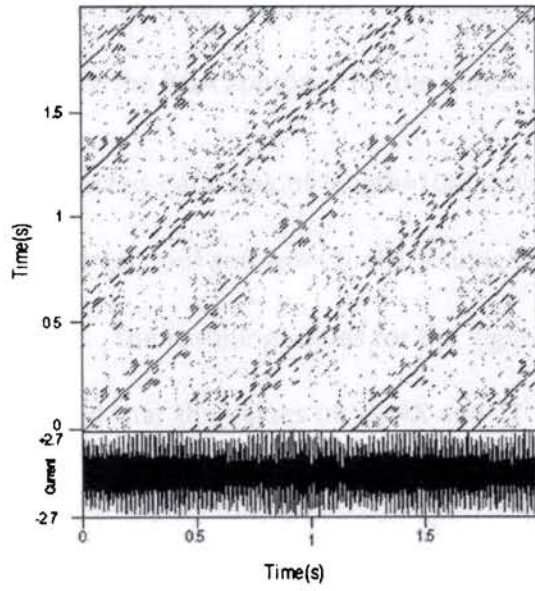
Table 6. 3. Calculated values for the threshold ϵ

	Current signal	Vibration Signal
Fresh Tool	10	7
Worn Tool	11	9

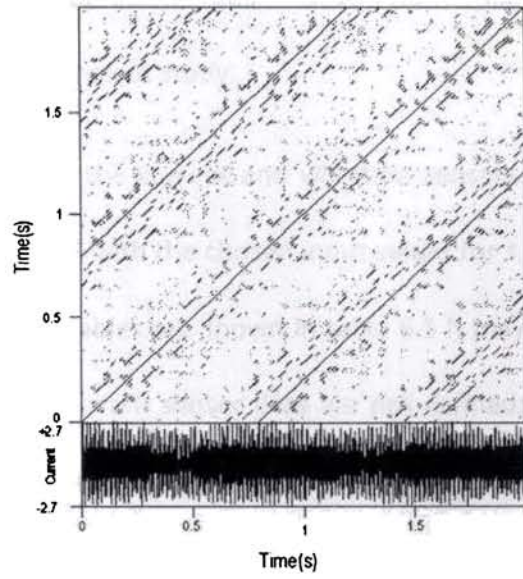
Table 6. 4. Chosen values for the threshold ϵ

	Current signal	Vibration Signal
Fresh Tool	11	9
Worn Tool	11	9

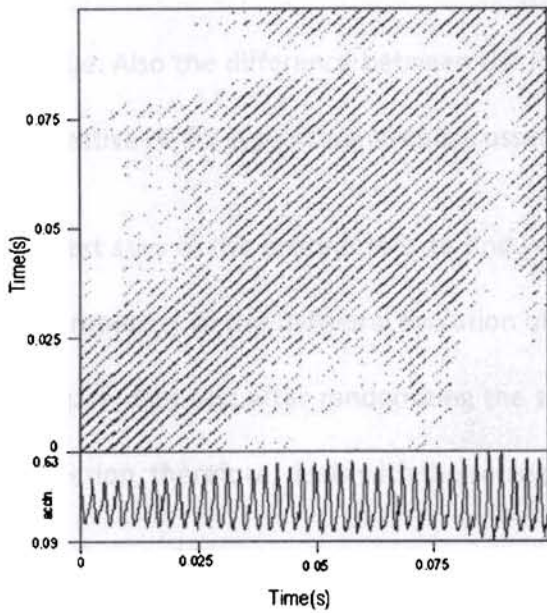
Sample data sets of length=1000 from current and vibration sensors, for the fresh tool and worn tool are now used to construct the RPs using the chosen input values for τ , m and ϵ . The output plots are shown in Figure 6.3. The RP axes are in time units.



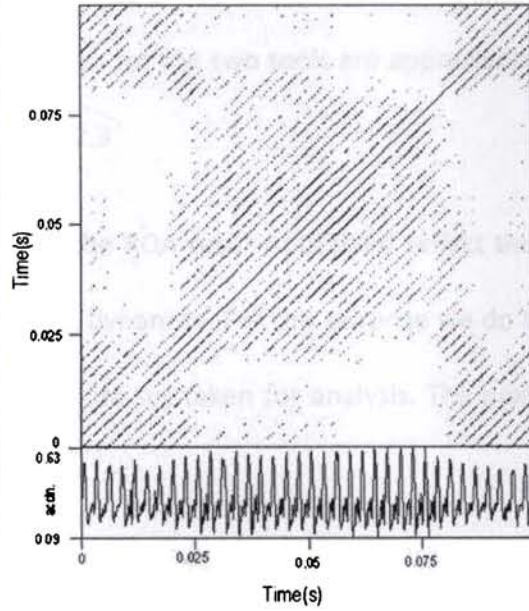
(a) Fresh tool- Current signal data



(b) Worn Tool- Current signal data



(c) Fresh tool-Vibration signal data



(d) Worn Tool-vibration signal data

Fig. 6.3. Recurrence plots of current and vibration signals data for system using fresh and worn tool.

Since the RPs itself does not contain any visually appreciable quantitative information we utilize the RQA approach for the purpose in the present study.

The selected data sets of length=1000 points, from the current and vibration sensors, for the fresh tool and worn tool are subjected to RQA with the chosen input values for τ , m and ϵ . The resulting values for the eight RQA variables are shown in table 6.5 It may be noted that the values of VMAX and TT for the current sensor data are not defined; this is due to the highly periodic nature of the current signal coupled with its low frequency at 50 Hz. This means that it is difficult to find vertical lines in RPs of current signal under the chosen construction criteria. Again, from the table it is found that as the tool wear takes place certain RQA variable values shows a definite trend to decrease its value. Also the difference between the RQA values for the two tools are appreciable irrespective of the type of signal as discussed in 6.1.2.3

The next step in the procedure is to find whether the RQA results obtained reflect the true properties of the temporal evolution of cutting dynamics. For this purpose we do a surrogate data test after randomizing the sample data set taken for analysis. The next sub section, therefore, deals with the surrogate data test.

6.1.2.2 *Surrogate Data Test*

Here, the actual intact data RQA results for the fresh tool and the worn tool are compared with the RQA results obtained after randomizing the same data points. It is found that this randomization effectively destroyed all the structures revealed under the input parameter values chosen earlier, as shown in Table 6.6. For example, with

other recurrence variables, percentage recurrence and percentage determinism dropped to around 0–5%. Furthermore, on examination, recurrence plots showed the homogeneous typology and did not resemble those for the actual intact data. Thus, it may be concluded that the results obtained under the present parameterization reflect true properties of the temporal evolution of cutting dynamics and contain a degree of deterministic structure.

Table 6.5 RQA values of current and vibration signals for system using fresh and worn tool.

	Fresh Tool	Worn Tool
<i>Current sensor signals</i>	Actual data, $\epsilon = 11$	Actual data, $\epsilon = 11$
Percent recurrence	3.491	2.386
Percent determinism	80.447	73.827
Linemax	406	597
Entropy	3.208	2.823
Trend	1.028	0.978
Percent Laminarity	0.00	0
Vmax	--	--
Traptime	--	--
<i>Vibration sensor signal</i>	Actual data, $\epsilon = 9$	Actual data, $\epsilon = 9$
Percent recurrence	2.625	1.033
Percent determinism	82.572	69.462
Linemax	179	98
Entropy	2.434	1.967
Trend	-6.390	0.498
Percent Laminarity	52.445	10.828
Vmax	4	3
Traptime	2.116	2.004

Table 6.6 - RQA values of current and vibration signals for system using fresh and worn tool, using both intact and randomized data sets

Fresh Tool	Current sensor signals	Actual data, $\epsilon = 11$	Randomized data, $\epsilon = 11$
	Percent recurrence	3.491	0.113
	Percent determinism	80.447	0.362
	Linemax	406	2
	Entropy	3.208	0
	Trend	1.028	0.060
	Percent Laminarity	0.00	0.725
	Vmax	--	--
	Traptime	--	--
	Vibration sensor signal	Actual data, $\epsilon = 9$	Randomized data, $\epsilon = 9$
	Percent recurrence	2.625	0.007
	Percent determinism	82.572	0.000
	Linemax	179	--
	Entropy	2.434	1
	Trend	-6.390	0.003
	Percent Laminarity	52.445	0.000
Vmax	4	1	
Traptime	2.116	--	
Worn Tool	Current sensor signals	Actual data, $\epsilon = 11$	Randomized data, $\epsilon = 11$
	Percent recurrence	2.386	0.162
	Percent determinism	73.827	0.000
	Linemax	597	--
	Entropy	2.823	--
	Trend	0.978	-0.007
	Percent Laminarity	0	0.506
	Vmax	--	--
	Traptime	--	--
	Vibration sensor signal	Actual data, $\epsilon = 9$	Randomized data, $\epsilon = 9$
	Percent recurrence	1.033	0.014
	Percent determinism	69.462	0.000
	Linemax	98	--
	Entropy	1.967	--
	Trend	0.498	-0.006
	Percent Laminarity	10.828	0.000
Vmax	3	--	
Traptime	2.004	--	

Table 6.7. RQA Variables – Mann-Whitney U test results

Recurrence Variable	Fresh Tool	Worn Tool	P (Two tailed)	Significance Level
<i>Current sensor signals</i>				
Percent recurrence	3.4910	2.3860	0.0140	Marginally significant
Percent determinism	80.447	73.827	0.0004	Highly Significant
Entropy	3.2080	2.8230	0.0045	Significantly different
<i>Vibration sensor signal</i>				
Percent recurrence	2.6250	1.0330	0.0130	Marginally significant
Percent determinism	82.572	69.462	0.0016	Significantly different
Entropy	2.4340	1.9670	0.0035	Significantly different

6.1.2.3 Mann-Whitney U Test

Now, to ascertain whether the differences seen in the calculated RQA variable values due to tool change, i.e. when the fresh tool is replaced by the worn tool, is by chance or otherwise the non parametric Mann-Whitney U test is carried out to find their statistical significance. The tests results (Table 6.7) shows that the difference in values between different sets that can arise by chance is by five per cent or less only in the case of percent recurrence, percent determinism and entropy whereas the remaining five are found to be not significantly different statistically . This is in contrast to the recent theoretical simulation study by Litak et al. [148] where the finding points to LMAX as the most conclusive variable in cutting dynamics, but in agreement with sensitiveness to Shannon’s information entropy.

6.1.2.4 RQA Episodic Test

An episodic test conducted on the full length of sample data sets to examine constancy of the significant RQA variables within the whole length of data (Figure 6. 4) Here an

epoch is designed to have a width of 400 data points and is made moving giving a 2 point data shift. Also, the figures show wide separations between the means of values of the recurrence variables suggesting of two distinct dynamics. This is explained by the source of the data; the upper graph in each is from a system using fresh tool whereas the second half is from a system using worn tool. This result corroborates and reiterates the Mann-Whitney U test outputs.

Finally, it is to be noted here that the above tests are conducted with constant input parameter values for both the data sets; fresh as well as worn tool. As a check, we have examined the effects on RQA variables if the calculated input parameter values were used in RQA. Since the representative values of worn tool test data have been used as the constant input parameters, it is sufficient to analyze the fresh tool signal data only, but with the calculated input parameter values for it, ie. for current signal $\tau=3$, for vibration signal $\tau=6$ and the corresponding values for m and ϵ are 3, 5 and 10,7. The RQA results with these input parameters indicate a 40-50% increase in percent recurrence value while other significant RQA variables; the percent determinism and entropy changes by only 1-2%. The change in percent recurrence is attributed to the fact that as the embedding dimension decreases from 5 to 3 along with a reduction in the threshold radius the mean distance is found to decrease by over 20%. This result justifies the assumption to use constant input parameter values for online detection, as it is found to have no trade-off in using instantly calculated values for the input parameters epoch by epoch.

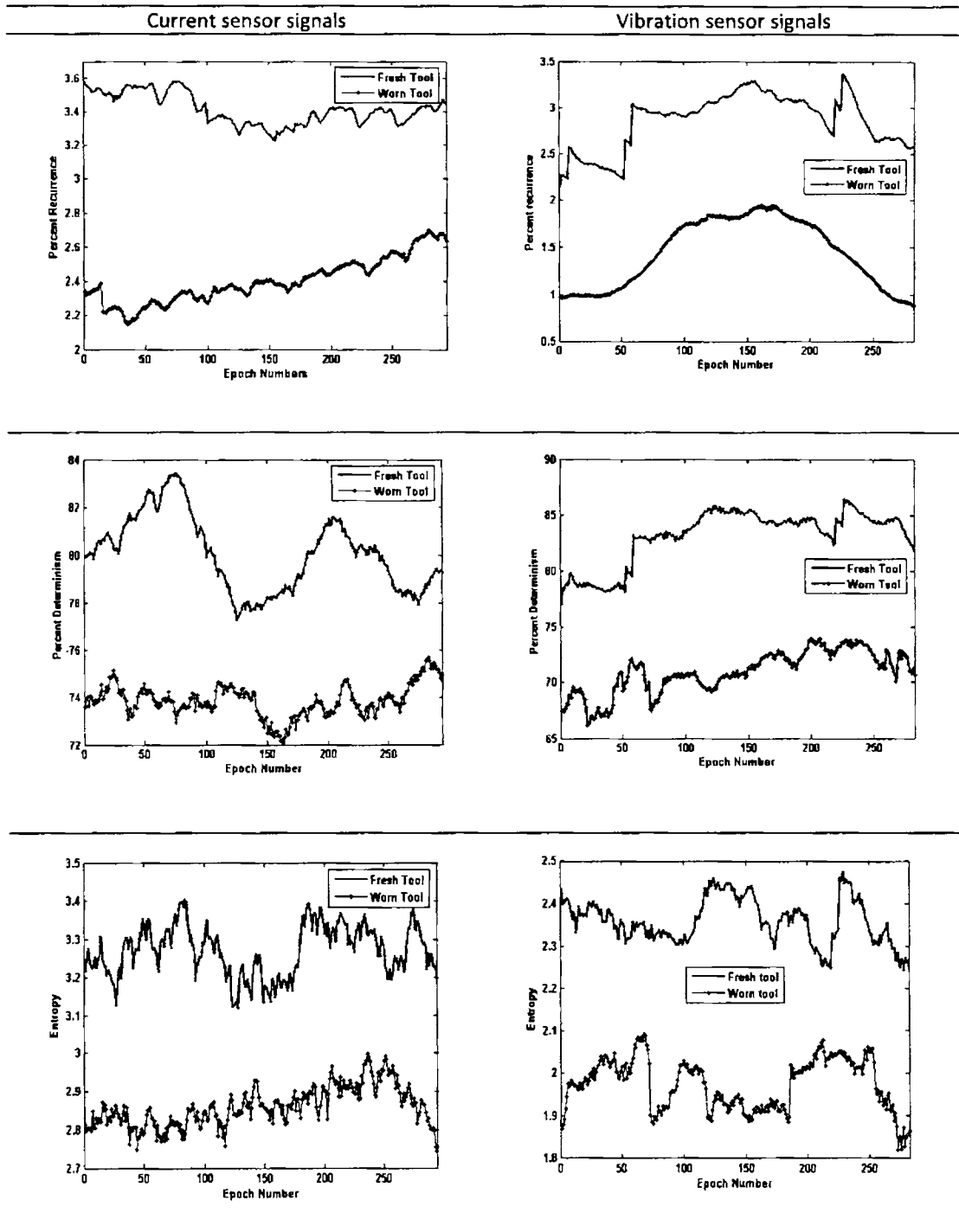


Fig. 6. 4 Episodic recurrence analysis of test signals.

6.1.2.5 *Observations*

- 1) The study has been initiated with an assumption that system output signals (e.g. vibration etc.) are much superior to system input signal (e.g. current drawn by the system) for analyzing the system dynamics. But, the present study could not establish such a distinction.
- 2) The surrogate data test shows that the results obtained are the true properties of the temporal evolution of the cutting process dynamics and contain a degree of deterministic structure. Moreover, the Mann-Whitney U test reveals that the results obtained are not due to some form of chance occurrence. This in essence means absence of any measurement error.
- 3) The Mann-Whitney U test categorically establishes the dependence of three RQA variables on tool wear; %DET, %REC and ENT which then emerge as the significant RQA variables in the study.
- 4) The wide separation between the mean values of the significant RQA variables representing the two conditions under study suggest that RQA can be an efficient tool in analyzing time series related to tool wear.

EXPERIMENT SET 2 - CHATTER

The RPs based method of analysis is found to be least affected by measurement or dynamic types of noise in the sensor data. Also the non-stationarity of data is seen to have little influence on the outcome of RQA. It is, therefore, very much likely that RQA variables can closely describe dynamical behavior of the cutting process under conditions of chatter than any other measures of nonlinearity which quite often is plagued by the above mentioned data characteristics. This has led us to the important assumption that the trends exhibited by RQA variables during chatter free-to-chatter regimes of cutting will be identical under any conditions or configurations of operation and therefore can be taken as characteristics of the dynamic response that can convey the chatter conditions reliably. Consequently this study explores applicability of the RQA methodology in detecting the transition from chatter free to chatter cutting during turning process.

Here two different experiments are carried out; Part-1 and Part-2. In Part-1 attempt is made to identify the sensitivity of the significant RQA variables to machine tool chatter and in Part-2 experiments are conducted to validate the nature of variation of the identified sensitive RQA variables when the cutting changes from chatter free to chatter in an actual situation.

6.2.1 Experiment Set 2 -Part 1

Sensitivity of the significant RQA variables to cutting dynamics during chatter free and chatter situations are examined here.

6.2.1.1 Experiments and Data Acquisition

The two regimes of cutting; the chatter free and the chatter cutting are created by performing turning on a work piece consisting of a stepped shaft of smaller diameter 47 mm and the larger diameter 50 mm along a length of 250 mm as shown in Figure 5.2. The machining job in the experiment involves reducing the work piece to a uniform rod of 46.6 mm cross section in a single pass of the tool from one end of the rod to the other. The feed direction is set along the axis of the work piece from smaller diameter to larger diameter. From the geometry it may be deduced that for the initial 125 mm length of the work piece the depth of cut have been 0.2 mm and for the remaining 125 mm it increased to 1.7 mm. The change from 0.2 mm to 1.7 mm has taken place abruptly at 125 mm length. This particular design ensured that the cutting have been chatter free for the first half where the depth of cut have been only 0.2 mm and when it suddenly increased to 1.7 mm the condition changed into chatter cutting for the

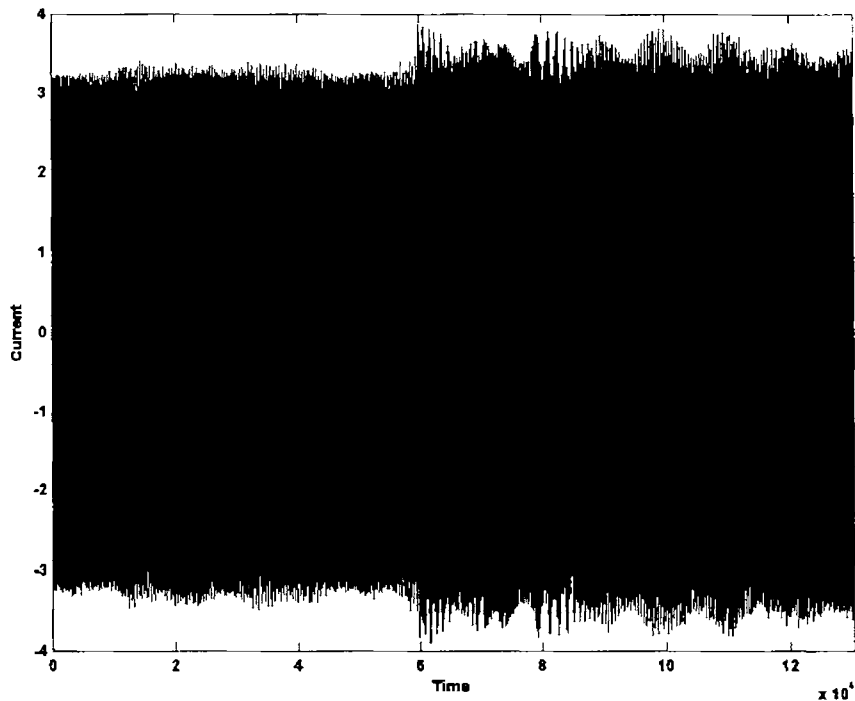


Fig. 6.5 Part-1 experimental time series

remaining half. This is because, for the second half portion of the work piece the speed and feed are the same as in the first portion but there is a considerable increase in the depth of cut at the 125 mm length.

In all the experiments under this section, the current sensor is made use of. Several trials of experiments are carried out under identical conditions and the corresponding time series of the sensor signals are recorded. When put into display all of them showed the same kind of variations. Besides, their mean values at arbitrarily selected points are examined and found to match each other ensuring repeatability.

A typical time series is shown in Figure 6.5. This data set is called Part-1 experimental time series. Not all the data points captured for one complete pass of cutting is shown

here, only the relevant portion from the continuous series is taken. The beginning 60000 data points on the plot represents 120 sec duration cut, i.e. on a 67.2 mm length immediately ahead of the 1.5 mm step on the 47 mm diameter portion of shaft and the remaining 70000 points represents 140 sec duration cut i.e. on a 78.4 mm length on the 50 mm diameter portion immediately following the step.

6.2.1.2 Data Analysis

The RQA of the experimental time series is performed after determining the phase space reconstruction parameters τ and m by using AMI and FNN methods. The threshold ϵ is chosen by analyzing the measure of recurrence point density [145] as percentage of maximum distance. The values for these parameters are calculated by analyzing the initial 120 sec duration of cut on the 67.2 mm length of the work piece.

The obtained values are shown in Table 6.8

Table 6.8. RQA input parameters for Part-1 experimental time series

Current Sensor Data			
Data set (Time series)	τ	m	ϵ
Part-1 experimental time series	3	3	23

In the episodic recurrence quantification analysis the significant RQA variables are computed for each epoch and presented in Figure 6.6. An epoch is designed to have a width of 512 data points and is made moving by giving a 128 point data shift resulting in total of 1014 epochs. Studying variations in the RQA variable values with changing epochs, these plots demonstrate heavy fluctuations in all the three RQA variable values between epoch numbers 468 and 610, without showing any definite trend. Beyond the

epoch 610 the volatility appears to settle down. It may be noted that, the change in depth of cut that has increased to 1.7 mm at the 1.5 mm step causes the operation to chatter cutting. This step is lying in epoch 468 in the analysis. Beyond this point the chatter conditions should prevail owing to the higher depth of cut where the speed and feed rates still remains the same as in chatter free cutting region, i.e. before that of the step.

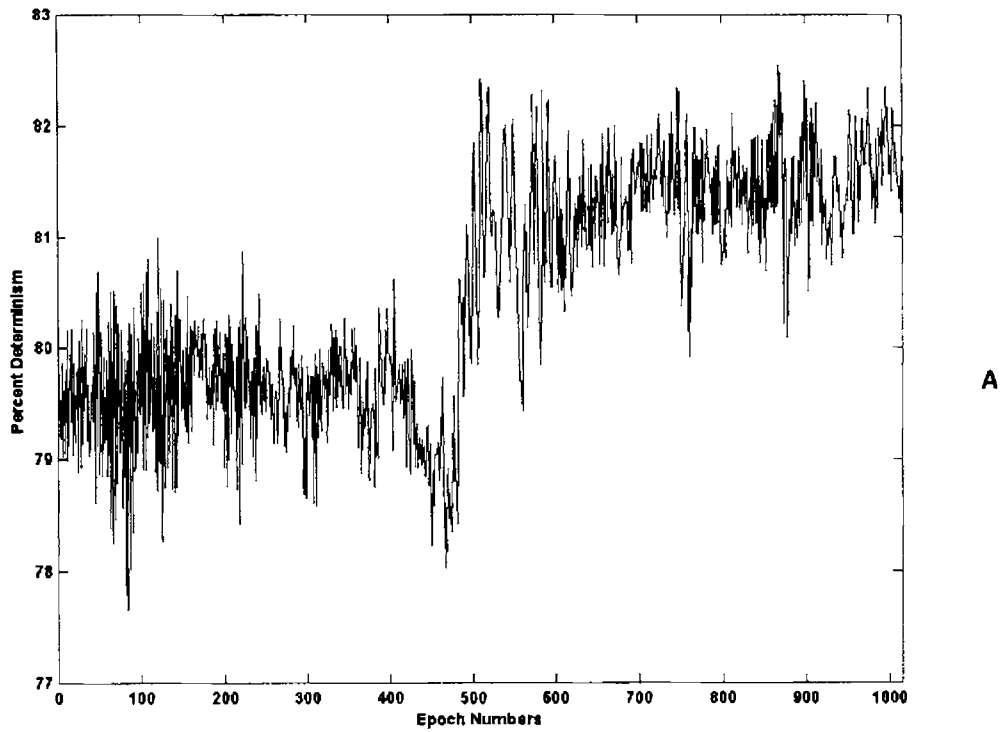
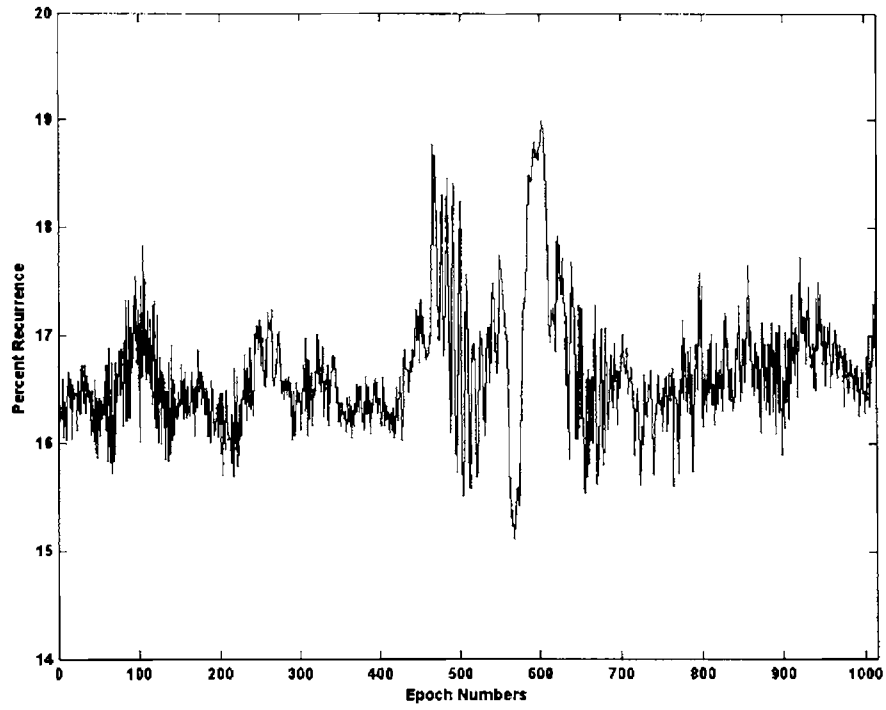
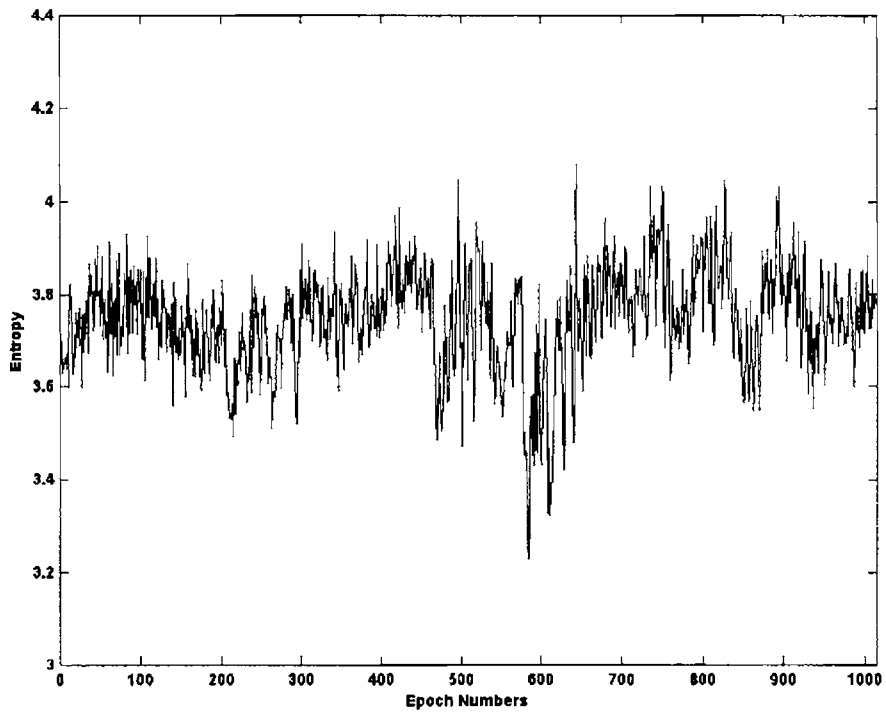


Fig. 6.6. RQA results for Part-1 experimental time series



B



C

Fig. 6.6. RQA results for Part-1 experimental time series

Moreover, it has already been reported that, in turning, at the transition from chatter-free cutting to chatter, a significant increase of determinism is usually observed [116,117]. Further, it is known that onset of chatter represents a transition from high-dimensional to low-dimensional dynamics. These findings come in support for the varying trends seen in plot of percent determinism (Figure 6.6.A). At the onset of chatter the percent determinism values, in general, shows an uptrend at a great rate before taking the values to a higher mean after considerable oscillations. From the figure it is clear that this RQA variable is much sensitive to chatter vibrations during cutting; a steady higher value of percent determinism is thus indicative of chatter as seen beyond epoch 468. The plot could thus vividly indicate the two regions of cutting. The other two variables; percent recurrence and entropy, on an average, assume constant values (Figures 6.6.B&C). Still these variables also show great fluctuations during the transition with the entropy showing a predominantly downtrend before reaching back. The foregoing discussion on RQA of Part-1 experimental time series reveals that the RQA variable percent determinism has a strong affinity to take lower values of percent determinism during chatter free cutting compared to chatter conditions.

6.2.2 Experiment Set 2 -Part 2

6.2.2.1 Experiments and Data Acquisition

In order to verify the sensitivity of the percent determinism to chatter as it sets in or during its occurrences, several experiments are conducted using a cylindrical work piece

of continuously varying cross-section (Figure 5.2-Part 2) and captured the sensor signals when the cutting is taking place. The work piece has an operating length of 250 mm. The diameters are 47 mm at one end and increased with a constant taper to 50 mm at the 250 mm length giving it a truncated conical shape. During experiments the speed (560 rpm), feed (0.06 mm per revolution) are maintained constant while the depth of cut is increased slowly but steadily from 0.2 mm to 1.7 mm. This is accomplished due to the shape of the work piece. This geometry is similar to the one used by Grabec [118] in his experiments reporting the capability of coarse grained entropy rate of the time series to detect onset of chatter. The sensor signals are recorded as Part-2 experimental time series for analysis.

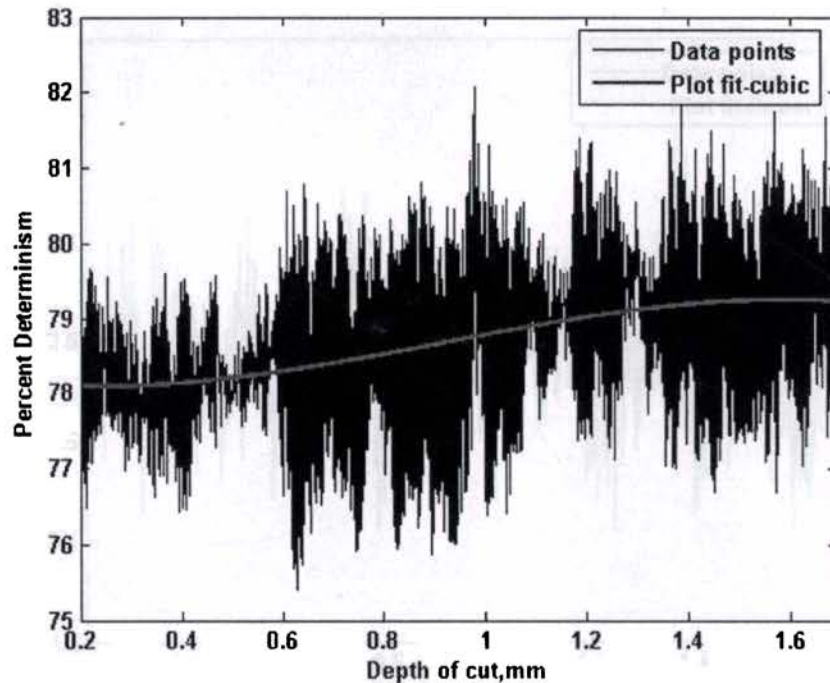
6.2.2.2 *Data Analysis*

The embedding parameters for Part-2 experimental time series and its threshold radius are found out as before and their values are listed in Table 6.9. The RQA outputs on the time series is carried out epoch by epoch with constant input parameters. The fluctuations in values of the three RQA variables with respect to depth of cut is shown in Figure 6.7

Table 6.9 RQA input parameters for Part-2 experimental time series

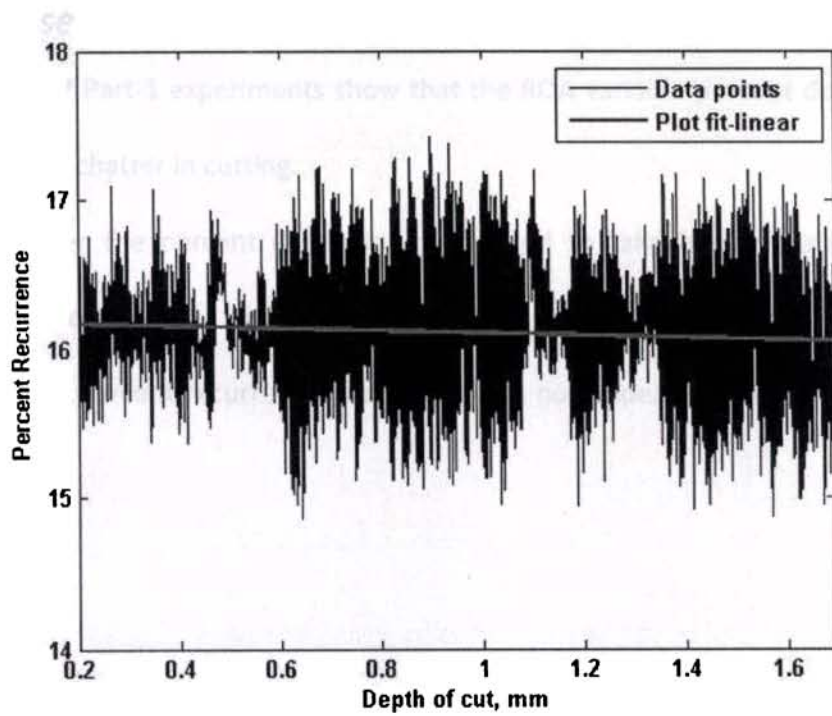
Current Sensor Data			
Data set (Time series)	τ	m	ϵ
Part-2 experimental time series	3	3	23

As expected the percent determinism remains constant up to a depth of cut of 0.45 mm (Figure 6.7.A) and afterwards it is seen increasing at a rapid rate. The plot data set that is fitted with a cubic spline exhibits this behavior. Comparing with the pattern in Figure 6.6.A, this upward trend that begins at 0.45 mm and developing afterwards can be attributed to chatter. The other two RQA variables, %REC and ENT, maintains almost constant mean values for all depth of cuts. Different trial samples of Part-2 experimental time series also gave exactly similar trends corroborating the sensitivity of percent determinism to chatter.

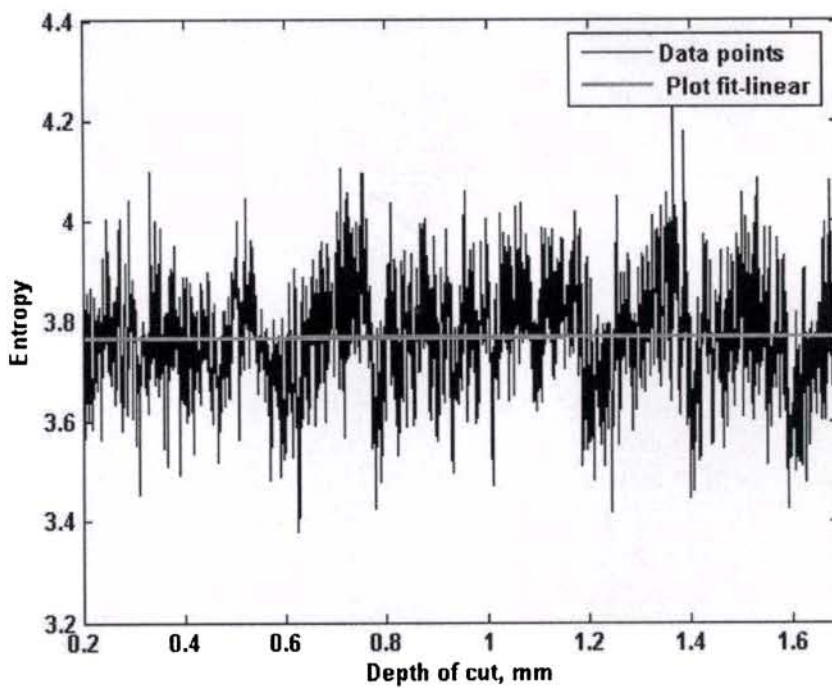


A

Fig. 6. 7 RQA variables - Set-2 experimental time series



B



C

Fig. 6.7 RQA variables - Set-2 experimental time series

6.2.2.3 *Observations*

- 1) The results of Part-1 experiments show that the RQA variable percent determinism is sensitive to chatter in cutting.
- 2) During chatter the percent determinism is found to take higher plateau values compared to chatter free conditions.
- 3) The variables percent recurrence and entropy do not appear to respond to chatter assertively.

Chapter 7 - Summary, Benefits and Future Directions

The focus of the thesis has been to investigate the applicability of RQA in metal cutting with specific objective to detect tool wear and chatter. This is a complex task, especially when information has to be deduced solely from sensor signals. Traditional methods do not address the issue of how to treat noise present in real-world processes and its non-stationarity. However, these issues are of great importance to machining process and system characterization, as the industry does not tolerate any spurious results. In an effort to get over these issues to the maximum possible, the RQA methodology is adopted. The performance of the results establishes the methodology to be viable for detection of tool wear and chatter. The key reason is that the dynamics of most machining process and systems are nonlinear and RQA can characterize them adequately. This work establishes that principles and practice of machining can be considerably benefited and advanced from using nonlinear dynamics and chaos theory.

In the following section the conclusions of the thesis based on the results obtained are summarized.

7.1 Summary

- 1) The work establishes that the input as well as output type signals can be used in RP based studies to analyze chaotic system dynamics for useful feature extraction. In a condition monitoring context this means that either of the signals can reliably transmit tool wear information.
- 2) The study reveals dependence of three RQA variables on tool wear; percent determinism, percent recurrence and entropy. Hence they are called significant RQA variables in RP based tool wear analysis.
- 3) As the wear on the tool flank increases the process is found to become dimensionally more complex. This substantiates the lower determinism obtained for the worn tool.
- 4) The wide separation between mean values of the significant RQA variables representing the two states of the tool under study suggest that RQA can be an efficient tool in time series analysis related to tool wear.
- 5) The fact that significant RQA variables assumes widely separated values for different quality tools is suggestive of this methodology to use as an efficient, dependent feature extraction methodology in a tool condition monitoring system under constancy of the underlying system parameters.

- 6) At the transition from chatter free to chatter, the RQA variable, percent determinism increases at a rapid rate before taking a higher plateau value, i.e. when chatter conditions prevail; percent determinism assumes a higher mean value compared to chatter free conditions. Thus a steady higher value of percent determinism is indicative of chatter.
- 7) Among the three significant RQA variables that are identified in the tool wear studies, only percent determinism emerge as a useful feature responding to chatter conditions conclusively.

7.2 Benefits

- 1) This method is robust against non-stationarity and noise in the signal leading to reliable results in comparison to other nonlinear measures.
- 2) The RQA variables can be derived very easily from a time series data at a significantly lesser cost since the data size and computational resource requirements are appreciably lower compared to other nonlinear time series analysis methodologies.
- 3) As feature extraction can be done reliably from even a small size data set as low as 500 data points, the computational time required for variable estimation is lower. This makes RP based approaches, RQA, an attractive feature extraction methodology that can be implemented in a condition monitoring system for quick retrieval of information from sensor signals.
- 4) The current sensor used is easy to use and is very cheap, in comparison to most other sensors. Also this can be fitted in the machine tool easily and is least affected by the harsh machining environment.

7.3 Contributions

- 1) New and efficient approach to detect tool wear and chatter in turning
- 2) Reported features are sensitive to tool wear and chatter
- 3) Operationalization of recurrence concept

7.4 Future directions

- 1) The studies may be repeated in a CNC machine using varied sensors.
- 2) Sensitivity of the significant RQA variables may be tested in high-speed machining.
- 3) Cross recurrence plots based studies may be conducted using an input signal and an output signal. The output signal can be from a dynamometer, accelerometer, an acoustic emission sensor or a microphone, while keeping the sampling rate same for both the signal types.

7.5 Conclusion

As evident in this work, the RQA methodology can be seen as a provider of quantitative decision support in condition monitoring of tool wear and chatter. Research efforts addressing the issues of noise and stationarity characteristics of sensor signals and moreover, the computational time demand for signal feature extraction, will advance not only machining principles and practice but also will render a fundamental contribution to the field of nonlinear dynamics.

List of Papers Submitted Based on This Thesis

International Journals (communicated)

- Rajesh V.G. and Narayanan Namboothiri V.N. , 2007, Utilizing recurrence quantification analysis for chatter detection in turning". *Mechanical systems and signal processing*,
- Rajesh V.G. and Narayanan Namboothiri V.N. , 2007, Recurrence quantification analysis of system signals for detecting tool wear in a lathe". *Physics Letters A*
- Rajesh V.G. and Narayanan Namboothiri V.N. , 2007, Flank wear detection of cutting tool wear in turning operation: application of nonlinear time series analysis". *Journal of Sound and Vibration*

International Conferences

- Rajesh V.G., Usha Nair and Narayanan Namboothiri V.N., 2006 Nov., " Time series analysis of audible sound signals during machining process", 36th International Conference Defektoskopie, Tabor, Czech Republic.
- Rajesh V.G. and Narayanan Namboothiri V.N, 2007 Jan., "Tool condition monitoring in a lathe using time series analysis of vibration signals." IISA Joint Statistical Meeting and International Conference, CUSAT, Cochin, India

- Rajesh V.G. and Narayanan Namboothiri V.N, 2007 Aug., “Recurrence plot-based approach for the detection of wear in lathe tool inserts”, International conference on advanced design and manufacturing, SIT, Virudhunagar, India
- Rajesh V.G. and Narayanan Namboothiri V.N, 2007 Aug., “Tool wear detection using recurrence quantification analysis of vibration sensor signals” International Conference on Modeling and Simulation, CIT, Coimbatore, India
- Rajesh V.G. and Narayanan Namboothiri V.N, 2007 Nov., “Drive motor current sensor based tool flank wear monitoring using chaos theory” 37th International Conference Defektoskopie, 2007, Praha, Czech Republic.

National Conference

- Rajesh V.G. and Narayanan Namboothiri V.N, 2007 June, “Application of the correlation dimension for tool condition monitoring” National Conference on Emerging Trends in Mechanical Engg, SVNIT, Surat, India.

References

1. J.U. Jeon, S.W. Kim, Optical flank wear monitoring of cutting tools by image processing, *Wear* 127 (1988) 207-217.
2. K.B. Pedersen, Wear measurement of cutting tools by computer vision, *International Journal of Machine and Tools Manufacturing* 30 (1) (1990) 131-139.
3. F. Giusti, M. Santochi and G. Tantussi, On-line sensing of flank and crater wear of cutting tools, *Annals of CIRP* 36 (1987) (1) 41-44.
4. R. Du, B. Zhang, W. Hungerford and T. Payor, Tool condition monitoring and compensation in finish turning using optical sensor, *Proceedings of symposium on Mechatronics, ASME Winter annual meeting (1993)*, pp 245-251.
5. A. Karthik, S. Chandra, B. Ramamoorthy and S. Das, 3D tool wear measurement and visualization using stereo imaging, *International Journal of Machine Tools and Manufacture* , 37 (1997) 1573-1581.
6. L. Gould, Sensing tool and drive element conditions in machine tools, *Sensor* (1988) 5-13 .
7. P.M. Lister, On-line measurement of tool wear, Ph.D. Thesis, Manufacturing and Machine Tools Division, Department of Mechanical Engineering, UMIST, Manchester, UK (1993)
8. S. E. Oraby and D. R. Hayhurst, Development of models for tool wear force relationships in metal cutting, *International Journal of Machine Tool and Manufacture*, 33, (1991) 125-138.
9. Y. Yao, X.D. Fang, and G. Arndt, Comprehensive tool wear estimation in finish-machining via multivariate time-series analysis of 3-D cutting forces," *CIRP Annals* 39 (1990) 57-60.

10. M. Bayramoglu and Ü. Dungal, A systematic investigation on the use of force ratios in tool condition monitoring for turning operations, Transactions of the Institute of Measurement and Control, London, (1998) 92-97.
11. T. Blum, and I. Inasaki, A study on acoustic emission from the orthogonal cutting process, ASME Journal of Engineering for Industry, Vol. 112 (1990) 203-211.
12. T. Moriwaki, and M. Tobito, A new approach to automatic detection of life of coated tool based on acoustic emission measurement, ASME Journal of Engineering for Industry 112 (1990) 212-218.
13. S.Y. Liang and D.A. Dornfield, Detection of cutting tool wear using time series modeling of acoustic emission signals, ASME Journal of Engineering for Industry 111 (1989) 199-205.
14. S. Kakade, I. Vijayaraghavan, and R. Krishnamoorthy, In-process tool wear and chipping monitoring in face milling operation using acoustic emission, Journal of Material Processing Technology, 44 (1994) 207-214.
15. S.B. Moshref, Cutting temperature as and approach to on-line measurement of tool wear," SME Technical Paper(1980), Paper No. IQ80-304
16. S.K. Choudhury and G. Bartarya, Role of temperature and surface finish in predicting tool wear using neural network and design of experiments, International Journal of Machine Tools and Manufacture, Volume 43, 7(2003) 747-753.
17. G.E. Derrico, A systems theory approach to modeling of cutting temperature with experimental identification, International Journal of Machine Tools and Manufacture, Volume 37, 2(1997) 149-158.
18. J. Lin, Inverse estimation of the tool-work interface temperature in end milling, International Journal of Machine Tools and Manufacture, Volume 35, 5(1995) 751-760.
19. F.R.S. Lima, A.R. Machado, S. Guts and G. Guimaraes, Numerical and experimental simulation for cutting temperature estimation using three dimensional inverse heat conduction technique, 3rd Conference on Inverse Problems in Engineering, Inverse problems in Engineering, Port Ludlow, WA, USA, Paper No. HT03 (1999)
20. D.E. Dimla Snr., Multivariate tool condition monitoring in a metal cutting operation using neural networks, Ph.D. thesis, School of Engineering and the Built Environment, The University of Wolverhampton, UK, (1998)

21. T.I. El-Wardany, D. Gao and M.A. Elbestawi, Tool condition monitoring in drilling using vibration signature analysis, *International Journal of Machine Tools and Manufacture* 36 (6) (1996) 687–711.
22. Y. Yao, X.D. Fang, G. Arndt, On-line estimation of groove wear in the minor cutting edge for finish machining, *Annals of the CIRP* 40 (1) (1991) 41–44.
23. L. Dan, J. Mathew, Tool wear and failure monitoring techniques for turning—a review, *International Journal of Machine Tools and Manufacture* 30 (4) (1990) 579–598.
24. J. Rotberg, S. Braun and E. Lenz, Mechanical signature analysis in interrupted cutting, *Annals of the CIRP* 36 (1) (1987) 249–252.
25. J. Rotberg, S. Braun, E. Lenz, Vibration generation models for cutting tool monitoring, *Diagnostics, Vehicle Dynamics and Special Topics—ASME Design Engineering Division* 18 (5) (1989) 1–6.
26. C.Y. Jiang, Y.Z. Zhang and H.J. Xu, In-process monitoring of tool wear stage by the frequency band-energy method, *Annals of the CIRP* 36 (1) (1987) 45–48.
27. D. Zhang, S. Dai, Y. Han and D. Chen, On-line monitoring of tool breakage using spindle current in milling, in: *1st Asia–Pacific and 2nd Japan–China International Conference Progress of Cutting and Grinding*, Shanghai, China, September(1994), pp. 270–276.
28. N. Constantinides, S. Bennett, An investigation of methods for on-line estimation of tool wear, *International Journal of Machine Tools and Manufacture* 27 (2) (1987) 225–237.
29. Xiaoli Li, Alexandar Djordjevich and Patri K. Venuvinod, Current-sensor-based feed cutting force intelligent estimation and tool wear condition monitoring, *IEEE Transactions on Industrial Electronics*, Volume 47, 3 (2000) 697 - 702.
30. G. O'Donnell, P. Young, K. Kelly and G. Byrne, Towards the improvement of tool condition monitoring systems in the manufacturing environment, *Journal of Materials Processing Technology*, 119 (2001) 133-139.
31. Karali Patraa, Surjya K. Pal and Kingshook Bhattacharyyaa, Artificial neural network based prediction of drill flank wear from motor current signals, *Applied Soft Computing*, Volume 7, 3 (2007) 929-935 .
32. K.F. Martin, J.A. Brandon, R.I. Grosvenor, A. and Owen, A comparison of in-process tool wear measurement methods in turning, in: *Proceedings International 26th MATADOR Conference*, Manchester, UK, 1986, pp. 289–296.

33. P.M. Lister and G. Barrow, Tool condition monitoring systems, in: Proceedings International 26th MATADOR Conference, Manchester, UK, 1986, pp. 271–288.
34. S. Kurada and C. Bradley, A review of machine vision sensors for tool condition monitoring, *Computers in Industry* 34 (1) (1997) 55–72.
35. D.C.D. Oguamanam, H. Raafat and S.M. Taboun, A machine vision system for wear monitoring and breakage detection of single-point cutting tools, *Computers in Industrial Engineering* 26 (3) (1994) 575–598.
36. A.A. Kassima, M.A. Mannan and Zhu Mian, Texture analysis methods for tool condition monitoring, *Image and Vision Computing*, Volume 25, 7(2007) 1080-1090 .
37. D. Cuppini, G. D’Enrrico, G. Rutelli, Tool image processing with application to unmanned metal-cutting, a computer vision system for wear sensing and failure detection, *SPIE 701* (1986) 416–422.
38. M. Shiraishi, Scope of in-process measurement, monitoring and control techniques in machining processes—Part 1: In-process techniques for tools, *Precision Engineering* 10 (4) (1988) 179–189.
39. A. Noori-Khajavi and R. Komanduri, Frequency and time domain analyses of sensor signals in drilling—I. Correlation with drill wear, *International Journal of Machine Tools and Manufacture* 35 (6) (1995) 775–793.
40. J.M. Zhou, M. Andersson and J.E. Stahl, A system for monitoring cutting tool spontaneous failure based on stress estimation, *Journal of Materials Processing Technology* 48 (1995) 231.
41. L.C. Lee, K.Y. Lam and X.D. Liu, Characterization of tool wear and failure, *Journal of Materials Processing Technology* 40 (1994) 143–153.
42. J.I. El Gomayel and K.D. Bregger, On-line tool wear sensing for turning operations, *ASME Transactions. Journal of Engineering for Industry* 108 (1986) 44–47.
43. S.K. Jetley and A. Gollajesse, Measuring tool wear using magnetism, in: Proceedings: Japan–USA Symposium Flexible Automation—A Pacific Rim Conference, July 11–18, Kobe, Japan, 1994, pp. 345–347.
44. N.H. Abu-Zahra, T.H. Nayfeh, Calibrated method for ultrasonic on-line monitoring of gradual wear during turning operations, *International Journal of Machine Tools and Manufacture* 37 (10) (1997) 1475–1484.

45. Dimla E. Dimla Snr., Sensor signals for tool-wear monitoring in metal cutting operations-a review of methods, *International Journal of Machine Tools and Manufacture* 40(2000) 1073-1098.
46. Steven Y. Liang, Rogelio L. Hecker and Robert G. Landers, Machining process monitoring and control: the state of art, *Journal of Manufacturing Science and Engineering* 126 (2004) 297-310
47. G. Byrne, D. Dornfeld, I. Inasaki, G. Ketteler, W. Ko"nig, R. Teti, Tool condition monitoring (TCM)—the status of research and industrial application, *Annals of CIRP* 44 (2) (1995) 541–567.
48. J. Tlusty, *Machine Dynamics, Handbook of High Speed Machining Technology*, New York Chapman and Hall, 1985, pp. 48-143.
49. F.W. Taylor, On the art of cutting metals. *Transactions of ASME* 28(1907) 331-350.
50. R.N. Arnold, The mechanism of tool vibration in the cutting of steel. in. *Proceedings of the Institution of Mechanical Engineers*, 154(4) (1946) 261-284.
51. S.A. Tobias, *Machine-Tool Vibration*, Blackie and Sons Ltd.: Glasgow, Scotland, 1965.
52. S.A. Tobias and W. Fishwick, The chatter of lathe tools under orthogonal cutting conditions. *Transactions of the ASME* 80 (1958) 1079.
53. S.A. Tobias and W. Fishwick, Theory of regenerative machine tool chatter. *The Engineer* (1958) 205.
54. J. Tlusty and M. Polocek, The stability of the machine-tool against self-excited vibration in machining. In *Proceedings of the International Research in Production Engineering Conference*, Pittsburgh, PA, ASME: New York, 1963, p. 465.
55. F. Koenisberger, J. Tlusty, *Machine Tool Structures-Vol. I: Stability Against Chatter*, Pergamon Press, 1967.
56. H. Merrit, Theory of self-excited machine tool chatter. *ASME Journal of Engineering for Industry*, 87 (4)(1965) 447-454.
57. R.L. Kegg, Cutting dynamics in machine tool chatter. *ASME Journal of Engineering for Industry*, 87 (4){1965) 464-470.
58. R. Shridar, R.E. Hohn and G. W. Long, A stability algorithm for the general milling process. *ASME Journal of Engineering for Industry* 90(1968) 330-334
59. N. H. Hanna and S.A. Tobias, A Theory of nonlinear regenerative chatter. *ASME Journal of Engineering for Industry*, 96(1974) 247-255.

60. J. Tlusty, W. Zaton and F. Ismail, Stability lobes in milling. *Annals of the CIRP*, 32 (1) (1983) 309-313.
61. G. Stepan, T. Inspenger and R. Szalai, Delay, parametric excitation and the nonlinear dynamics of cutting process, *International Journal of Bifurcation and Chaos*, Vol. 15(9) (2005) 2783-2798.
62. J. Tlusty, Analysis of the state of research in cutting dynamics. *CIRP Annals*, 27(1978) 583-589.
63. I. Minis, T. Yanushevsky, R. Tembo and R. Hocken, Analysis of linear and nonlinear chatter in milling. *Annals of the CIRP*, 39 (1) (1990) 459-462.
64. S. Smith and J. Tlusty, An overview of modeling and simulation of the milling process, *ASME Journal of Engineering for Industry*, 113 (1991) 169-175.
65. Y. Altintas and E. Budak, Analytical prediction of stability lobes in milling, *Annals of the CIRP*, 44 (1) (1995) 357-362.
66. A. H. Nayfeh, C.M. Chin and J. Pratt, Applications of perturbation methods to tool chatter dynamics, *Dynamics and Chaos in Manufacturing Processes*, Wiley, New York, 1997.
67. G. Stepan and T. Kalmar-Nagy, Nonlinear regenerative machine tool vibrations, In *Proceedings of the 16th Biennial Conference on Mechanical Vibration and Noise*, ASME Design Engineering Technical Conferences, Sacramento, CA, September 14-17, 1997; DETC97/VIB-4021.
68. E. Budak and Y. Altintas, Analytical prediction of chatter stability conditions for multi-degree of freedom systems in milling, Part I: Modeling, Part II: Applications. *Journal of Dynamic Systems, Measurement and Control*, 120(1998) 22-36.
69. J. Pratt, M.A. Davies, C.J. Evans, and M. Kennedy, Dynamic interrogation of a basic cutting process. *Annals of the CIRP*, 48 (1) (1999) 39-42.
70. S. Smith and J. Tlusty, Update on high-speed milling dynamics, *ASME Journal of Engineering for Industry*, 112(1990) 142-149.
71. T. Kalmar-Nagy, J.R. Pratt, M.A. Davies, and M. Kennedy, Experimental and analytical investigation of the subcritical instability in metal cutting. In *Proceedings of the 17th Biennial Conference on Mechanical Vibration and Noise*, ASME Design and Technical Conferences, Las Vegas, NV, September 12-16, 1999.

72. B. Roa and Y.C. Shin, A comprehensive dynamic cutting force model of chatter prediction in turning. *International Journal of Machine Tools and Manufacture*, 39 (10) (1999) 1631-1654.
73. M. Davies and B. Balachandran, Impact dynamics in milling of thin-walled structures. *Nonlinear dynamics*, 22 (2000) 375-392.
74. W.T. Corpus and W.J. Endres, A high order solution for the added stability lobes in intermittent machining. In *Proceeding of the Symposium on Machining Processes*, Orlando, FL; MED-11, 871-878.
75. M. Fofana and S. Bukkapatnam, A Nonlinear model of machining dynamics, In *Proceedings of the 18th Biennial Conference on Mechanical Vibration and Noise*, ASME Design Engineering Technical Conferences, Pittsburgh, PA, September 9-13, 2001.
76. B. Balachandran, Nonlinear dynamics of milling process, *Philosophical Transactions of the Royal Society of London A*, 359 (2001) 793-819.
77. P.V. Bayly, J.E. Halley, B.P. Mann and M.A. Davies, Stability of interrupted cutting by temporal finite element analysis, In *Proceedings of the 18th Biennial Conference on Mechanical Vibration and Noise*, ASME Design Engineering Technical Conferences, September 9-13, 2001, Pittsburgh, PA.
78. T. Insperger and G. Stepan, Semi-discretization method for delayed systems, *International Journal of Numerical Methods in Engineering*, 55(5)(2002) 503-518.
79. P. Bayly, J. Halley, B. Mann and M. Davies, Stability of interrupted cutting by temporal finite element analysis, In *Proceedings of the 18th Biennial Conference on Mechanical Vibration and Noise*, ASME Design Engineering Technical Conferences, Pittsburgh, PA, September 9-13, 2001
80. P. Bayly, T. Schmitz, D. Peters, B. Mann and G. Stepan, Insperger, T. effects of radial immersion and cutting direction on chatter instability in end-milling, In *Proceedings of ASME International Mechanical Engineering Congress and Exposition*, New Orleans, LA, 2002.
81. S. Jensen and Y. Shin, Stability analysis in face milling operations, Part 1: Theory of Stability Lobe Prediction. *Journal of Manufacturing Science and Engineering*, 121 (4) (1999), 600-605.
82. T. Delio, J. Tlustý and S. Smith, Use of audio signals for chatter detection and control, *ASME Journal of Engineering for Industry* 114 (1992) 145-157.

83. Y. Altintas and P.K. Chan, In-process detection and suppression of chatter in milling, *International Journal of Machine Tools and Manufacture*, Volume 32 (1992) 329-347.
84. Y.S. Tarang and T.C. Li, Detection and suppression of drilling chatter, *International Journal of Dynamic Systems, Measurement and Control*, 116 (1994) 729-734.
85. T. Bailey, Y. Ruget, A. Spence and M.A. Elbestawi, Open-architecture controller for Die and Mould Machining, *American Control Conference, Seattle, Washington, 1995*, pp. 194-199.
86. X. Q. Li, Y. S. Wong and A. Y. C. Nee, Tool wear and chatter detection using the coherence function of two crossed accelerations, *International Journal of Machine Tools and Manufacture*, Volume 37, 4 (1997) 425-435
87. E. Soliman and F. Ismail, Chatter detection by monitoring spindle drive current, *International Journal of Advanced Manufacturing Technology*, 13(1997) 27-34.
88. S. Bukkapatnam, A. Lakhtakia and S. Kumara, Analysis of sensor signals shows turning on a lathe exhibits low-dimensional chaos, *Physical Review E* 52 (1995) 2375-2387.
89. S. Doi and S. Kato, Chatter vibrations of lathe tools, *Transactions of ASME*, 78 (1956) 1127-1134
90. J. Tlustý and F. Ismail, Basic non-linearity in machining chatter. *CIRP Ann. Manufacturing Technol.* 30 (1981) 299-304.
91. I. Grabec, Chaos generated by the cutting process, *Physics Letters A* 117(1986) 384-386.
92. I. Grabec, Chaotic dynamics of the cutting process, *International Journal of Machine Tools and Manufacture*, 28 (1988) 19-32.
93. E. Marui, S. Kato, M. Harashimoto and T. Yamada, The mechanism of chatter vibrations in a spindle work piece system: Part 2 – Characteristics of dynamic cutting force and vibration energy, *ASME Journal of Engineering for Industry* 110 (1988) 242-247.
94. J. Gradisek, E. Govekar and I. Grabec, A chaotic cutting process and determining optimal cutting parameter using neural networks, *International Journal of Machine Tools and Manufacture*, 36 (1996) 1161-1172.
95. M. Wiercigroch and A.H.D. Cheng, Chaotic and stochastic dynamics of orthogonal metal cutting, *Chaos, Solitons & Fractals* 8 (1997) 715-726.
96. J. Warminski, G. Litak, J. Lipski, M. Wiercigroch and M.P. Cartmell, Vibrations in regenerative cutting process synthesis of nonlinear dynamical systems, In: Lavendelis, E.

- and Zakrzhevsky, M. (eds), *Solid Mechanics and its Applications* Vol. 73, Kluwer Academic Publishers, Dordrecht, 2000, pp. 275–283.
97. J. Warmiński, G. Litak, M.P. Cartmell, R. Khanin and M. Wiercigroch, Approximate analytical solutions for primary chatter in the nonlinear metal cutting model, *International Journal of Sound and Vibration* 259 (2003) 917–933.
 98. G. Litak, J. Warmiński and J. Lipski, Self-excited vibrations in cutting process, In *Proceedings of the 4th Conference on Dynamical Systems – Theory and Applications*, Łódź, Poland, December 1997. pp. 193–197.
 99. J.R. Pratt and A.H. Nayfeh, Design and modelling for chatter control, *Nonlinear Dynamics*, 19 (1999) 49–69.
 100. G. Stepan and T. Kalmar-Nagy, Nonlinear regenerative machine tool vibrations, in: *Proceedings of DETC'97*, Sacramento, California, September 1997.
 101. D.B. Marghitu, B.O. Ciocirlan and N. Craciunoiu, Dynamics in orthogonal turning process, *Chaos, Solitons & Fractals* 12 (2001) 2343–2352.
 102. F.C. Moon and T. Kalmar-Nagy, Nonlinear models for complex dynamics in cutting materials, *Phil. Transactions of the Royal Society of London A* 359 (2001) 695–711.
 103. I.N. Tansel, C. Erkal, T. Keramidas, The chaotic characteristic of three dimensional cutting, *International Journal of Machine Tools and Manufacture*, 32 (1992) 811–827.
 104. T. Kalmár-Nagy and F. C. Moon, *Mode-coupled regenerative machine tool vibrations*, *Nonlinear Dynamics of Production Systems*, Wiley-VCH, Berlin, 2004, pp. 129-149
 105. P.L.B. Oxley and W.F. Hastings, Predicting the strain rate in the zone of intense shear in which the chip is formed in machining from the dynamic flow stress properties of the work material and the cutting conditions. *Proceedings of the Royal Society of London, A* 356 (1977) 395-410.
 106. M. Johnson, *Nonlinear differential equations with delay as models for vibrations in the machining of metals*. PhD thesis, 1996, Cornell University.
 107. M. Johnson and F.C. Moon, Experimental characterization of quasiperiodicity and chaos in a mechanical system with delay, *International Journal of Bifurcation and Chaos* 9(1999) 49-65.
 108. H. Abarbanel, *Analysis of observed chaotic data*, 1996, Springer.
 109. B. Berger, M. Rokni and I. Minis, The nonlinear dynamics of metal cutting. *International Journal of Engineering Science*, 30(1992) 1433-1440.

110. B. Berger, I. Minis, Y. Chen, A. Chavali and M. Rokni, Attractor embedding in metal cutting, *International Journal of Sound and Vibration* 184 (1995) 936-942.
111. I. Minis and B.S. Berger, Modelling, analysis, and characterization of machining dynamics, In *Dynamics and Chaos in Manufacturing Processes* (ed. F. C. Moon), Wiley, 1998, pp. 125-163.
112. S.T.S. Bukkapatnam, Compact nonlinear signal representation in machine tool operations, In *Proc. 1999 ASME Design Engineering Technical Conference, Las Vegas, 1999, NV, USA*.
113. S.T.S. Bukkapatnam, A. Lakhtakia, S. Kumara and G. Satapathy, Characterization of nonlinearity of cutting tool vibrations and chatter. In *ASME Symp. on Intelligent Manufacturing and Material Processing*, vol. 69, 1995, pp. 1207-1223.
114. F.C. Moon, Chaotic dynamics and fractals in material removal processes. In *Nonlinearity and chaos in engineering dynamics* (ed. J. Thompson & S. Bishop), 1994, pp. 250-37. Wiley.
115. F.C. Moon and H. Abarbanel, Evidence for chaotic dynamics in metal cutting, and classification of chatter in lathe operations. In *Summary Report of a Workshop on Nonlinear Dynamics and Material Processes and Manufacturing* (ed. F. C. Moon), Institute for Mechanics and Materials, 1995, pp. 11-12, 28-29.
116. J. Gradisek, E. Govekar and I. Grabec, Time series analysis in metal cutting: chatter versus chatter-free cutting. *Mech. Sys. Signal Proc.* 12(1998) 839-854.
117. J. Gradisek, E. Govekar and I. Grabec, Using coarse grained entropy rate to detect chatter in cutting, *Journal of sound and vibration*, 214 (1998) 941-952,
118. I. Grabec, J. Gradisek and E. Govekar, A new method for chatter detection in turning. *CIRP Annals.* 48(1) (1999) 29-32.
119. H. G. Schuster, *Deterministic chaos*, VCH, Weinheim (1989).
120. E. Ott, *Chaos in dynamical systems*, Cambridge University Press, Cambridge (1993).
121. S. H. Strogatz, *Nonlinear dynamics and chaos*, Addison-Wesley, Massachusetts (1994).
122. H. Kantz and T. Schreiber, *Nonlinear time series analysis*, Cambridge University Press, Cambridge (1997).
123. H. D. I. Abarbanel, *Analysis of observed chaotic data*, Springer, New York (1996).
124. J. C. Sprott, *Chaos and time-series analysis*, Oxford University Press, Oxford (2003).
125. M. Small, *Applied nonlinear time series analysis*, World Scientific, Singapore (2005).

126. A. M. Fraser and H. L. Swinney, Independent coordinates for strange attractors from mutual information, *Physical Review A* 33 2 (1986) 1134–1140.
127. M. B. Kennel, R. Brown, and H. D. I. Abarbanel, Determining embedding dimension for phase-space reconstruction using a geometrical construction, *Physics Review A* 45 (1992) 3403.
128. N.H. Packard, J.P. Crutchfield, J.D. Farmer et al., Geometry from a time series, *Physical Review Letters* 45 (1980) 712-716
129. F. Takens, Detecting strange attractors in turbulence, *Dynamical Systems and Turbulence*, Warwick, Lecture Notes in Mathematics 898, Springer-Verlag, (1981) 366-381
130. T. Sauer, J.A. Yorke, and M. Casdagli, Embedology, *Journal of Statistical Physics* 64 (1991) 579-616
131. A. M. Fraser and H. L. Swinney, Independent coordinates for strange attractors from mutual information, *Physical Review A* 33 (1986) 1134-1140
132. R. Shaw, Strange attractors, Chaotic behavior and information flow. *Z. Naturforsch.*, 36a (1981) 80-112.
133. K. Judd and L. Smith, Indistinguishable states-perfect model scenario , *Physica D*, 151 (2001) 224-242
134. J.D. Farmer, E.Ott and J. A Yorke, The dimension of chaotic attractors, *Physica D*, 7 (1983) 153-180
135. J. Theiler, Estimating fractal dimension, *Journal of Optical Society of America*, 7 (1990) 1055-1073.
136. M. Perc, Introducing nonlinear time series analysis in undergraduate courses, *Fizika A (Zagreb)* 15 (2) (2006) 91–112
137. J.D. Reiss, The analysis of chaotic time series, Ph.D. thesis, Georgia Institute of Technology (2001)
138. H. Poincare, Sur la probleme des trois corps et les équations de la dynamique, *Acta Mathematica* 13 (1890) 1–271
139. J.P. Eckmann, S.O. Kamphorst, D. Ruelle, Recurrence Plots of Dynamical Systems, *Europhysics Letters*, 5 (1987) 973–977

140. N. Marwan, Encounters With Neighbors - Current developments of concepts based on recurrence plots and their applications, Ph.D. Thesis, University of Potsdam, ISBN 3-00-012347-4 (2003)
141. N. Marwan, N. Wessel, U. Meyerfeldt, A. Schirdewan and J. Kurths, Recurrence plot based measures of complexity and its application to heart rate variability data, *Physical Review E* 66 (2) (2002) 026702
142. J.P. Zbilut and C.L. Webber Jr., Embeddings and delays as derived from quantification of recurrence plots, *Physics Letters A* 171 (3-4) (1992) 199-203.
143. C.L. Webber Jr. and J.P. Zbilut, Dynamical assessment of physiological systems and states using recurrence plot strategies, *Journal of Applied Physiology* 76 (2) (1994) 965-973.
144. L.L. Trulla, A. Giuliani, J.P. Zbilut and C.L. Webber Jr., Recurrence quantification analysis of the logistic equation with transients, *Physics Letters A* 223 (4) (1996) 255-260.
145. C.L. Webber Jr. and J.P. Zbilut, Recurrence quantification analysis of nonlinear dynamical systems, *Tutorials in contemporary nonlinear methods for the behavioral sciences*, (Chapter 2, pp. 26-94), M.A. Riley, G. Van Orden, eds. Retrieved December 1 (2004).
146. C.L. Webber Jr., M.A. Schmidt and J.M. Walsh, Influence of isometric loading on biceps EMG dynamics as assessed by linear and nonlinear tools, *Journal of Applied Physiology*, 78 (1995) 814-822.
147. H.B. Mann and D.R. Whitney, On a test of whether one of two random variables is stochastically larger than the other, *Annals of Mathematical Statistics*, 18 (1947) 50-60.
148. G. Litak, A. Syta, N. Marwan and J. Kurths, Dynamics of a cutting process by recurrence plots, Second international workshop on recurrence plots, Siena, Italy, 2007

Appendix 1

Mathematical Construction of the Recurrence Matrix

RQA employs the method of time delays to embed experimental data into higher dimensions. Explicit examples of how distance matrices (DM) and recurrence matrices (RM) are constructed for Euclidean, maximum, and minimum norms are detailed below for a contrived time-series vector $\{x(j)\}$ with 29 elements.

$$\{x(j)\} = [3.7, 9.2, 2.1, -5.4, 0.0, -10.9, 9.2, 3.1, 1.7, 1.8, -0.3, -4.9, 2.7, 3.5, 7.5, -9.9, -9.9, -4.7, 1.3, 2.7, 7.6, 3.9, 7.3, 8.0, 0.3, -1.9, 5.1, 8.8, 8.2]$$

For $\tau=8$, $m=4$, the following 5 time-delay vectors are constructed:

$$X(1) = [+3.7, +1.7, -9.9, +0.3]$$

$$X(2) = [+9.2, +1.8, -4.7, -1.9]$$

$$X(3) = [+2.1, -0.3, +1.3, +5.1]$$

$$X(4) = [-5.4, -4.9, +2.7, +8.8]$$

$$X(5) = [+0.0, +2.7, +7.6, +8.2]$$

Comparison of the 5 vectors constructs a single 5×5 recurrence matrix of distances for each of the 3 norm types. For example, the Euclidean distance between vectors $X(4)$ and $X(5)$ is calculated as follows:

$$DM (L_2(i=4, j=5)) = \sqrt{(-5.4 - 0.0)^2 + (-4.9 - 2.7)^2 + (2.7 - 7.6)^2 + (8.8 - 8.2)^2} = 10.549.$$

To compute the maximum and minimum distances between vectors $X(4)$ and $X(5)$ the vectors are compared element by element.

$$|-5.4 - 0.0| = 5.4$$

$$|-4.9 - 2.7| = 7.6 \text{ (largest difference)}$$

$$|2.7 - 7.6| = 4.9$$

$$|8.8 - 8.2| = 0.6 \text{ (smallest difference)}$$

By definition, maximum and minimum distances are simply the maximum and minimum differences, respectfully.

$$DM (L_{\infty} (i = 4, j = 5)) = 7.6$$

$$DM (L_1 (i = 4, j = 5)) = 0.6$$

This procedure is repeated for each cell, giving the following results for $DM(i, j)$. Only the distances in the upper triangle are shown since the lower half is perfectly symmetrical. Note that the central diagonal is designated by 0.00 distances (vector identity matches).

$$DM(L_2) =$$

$$[1,5]=19.58; [2,5]=18.41; [3,5]=7.92; [4,5]=10.55; [5,5]=0.00$$

$$[1,4]=18.90; [2,4]=20.67; [3,4]=9.65; [4,4]=0.00$$

$$[1,3]=12.45; [2,3]=11.83; [3,3]=0.00$$

$$[1,2]=7.88; [2,2]=0.00$$

$$[1,1]=0.00$$

$DM(L_{\infty}) =$

[1,5]=17.50; [2,5]=12.30; [3,5]=6.30; [4,5]=7.60; [5,5]=0.00

[1,4]=12.60; [2,4]=14.60; [3,4]=7.50; [4,4]=0.00

[1,3]=11.20; [2,3]=7.10; [3,3]=0.00

[1,2]=5.50; [2,2]=0.00

[1,1]=0.00

$DM(L_1) =$

[1,5]=1.00; [2,5]=0.90; [3,5]=2.10; [4,5]=0.60; [5,5]=0.00

[1,4]=6.60; [2,4]=6.70; [3,4]=1.40; [4,4]=0.00

[1,3]=1.60; [2,3]=2.10; [3,3]=0.00

[1,2]=0.10; [2,2]=0.00

[1,1]=0.00

These distances are all expressed in absolute units and can be retained as such or *RM* distances are normalized to the mean distance of the *RM* by dividing each cell by the absolute mean distance and multiplying by 100. All central diagonal values of zero are excluded from the calculation of mean distance.

DM mean distance (L_2) = 13.783 = 100.0%

DM mean distance (L_{∞}) = 10.220 = 100.0%

DM mean distance (L_1) = 2.310 = 100.0%

The rescaling can also be done by normalizing the DM distances to the maximum distance of the DM by dividing each cell by the absolute maximum distance and multiplying by 100. Be careful not to confuse max distance and max norm, which are different.

$$DM \text{ max distance } (L_2) = 20.671 = 100.0\%$$

$$DM \text{ max distance } (L_\infty) = 17.500 = 100.0\%$$

$$DM \text{ max distance } (L_1) = 6.700 = 100.0\%$$

Recurrence matrices are derived from distance matrices by setting a RADIUS threshold. As shown below, the Heaviside function assigns values of 0 or 1 to array elements. The RADIUS parameter is always relative to the calculated max distance, whether it be expressed in absolute units or relative units. Only those distances in $RM(i, j)$ equal to or less than the RADIUS are defined as recurrent points at coordinates (i, j) .

$$RM (L_2 \text{ with RADIUS of } 8.0) =$$

$$[1,5]=0; [2,5]=0; [3,5]=1; [4,5]=0; [5,5]=1$$

$$[1,4]=0; [2,4]=0; [3,4]=0; [4,4]=1$$

$$[1,3]=0; [2,3]=0; [3,3]=1$$

$$[1,2]=1; [2,2]=1$$

$$[1,1]=1$$

$$RM (L_\infty \text{ with RADIUS of } 12.3) =$$

$$[1,5]=0; [2,5]=1; [3,5]=1; [4,5]=1; [5,5]=1$$

$$[1,4]=0; [2,4]=0; [3,4]=1; [4,4]=1$$

$$[1,3]=1; [2,3]=1; [3,3]=1$$

$$[1,2]=1; [2,2]=1$$

[1,1]=1

RM (L_1 with RADIUS of 1.2) =

[1,5]=1; [2,5]=1; [3,5]=0; [4,5]=1; [5,5]=1

[1,4]=0; [2,4]=0; [3,4]=0; [4,4]=1

[1,3]=0; [2,3]=0; [3,3]=1

[1,2]=1; [2,2]=1

[1,1]=1

RQA looks for patterns among these recurrent points, and this need not/must not be done manually (too subjective). Objective pattern recognition algorithms are written into the many recurrence programs to define the RQA variables %REC, %DET, ENT, LMAX, TND, %LAM, VMAX and TT.

APPENDIX 2

Mann-Whitney U test – Example Problem

The size of leaves taken from bramble bushes were measured to see if there is a difference between the size of the leaves growing in full sunlight and those growing in the shade.

	Width of leaf / cm							
Sunlight	6.0	4.8	5.1	5.5	4.1	5.3	4.5	5.1
Shade	6.5	5.5	6.3	7.2	6.8	5.5	5.9	5.5

The Mann-Whitney U-test is chosen because the sample size is so small it is not clear if these are samples taken from normally distributed data.

1. Set up the Null Hypothesis: There is no difference between the leaves taken from the sunlit bramble and the shaded bramble.

Alternative Hypothesis: There is a difference between the leaves taken from the sunlit bramble and the shade bramble.

2. Let k_1 be the size of the smallest sample and k_2 be the size of the biggest sample.
In this example both are of the same size so it does not matter which one is chosen.

$$k_1 = 8 \text{ and } k_2 = 8$$

3. Rank all the values for both samples from the smallest (=1) to the largest. Set them up as shown in the table below.

Sunlight	Rank	Rank	Shade
4.1	1		
4.5	2		
4.8	3		
5.1	4.5		
5.1	4.5		
5.3	6		
5.5	8.5		
		8.5	5.5
		8.5	5.5
		8.5	5.5
		11	5.9
6.0	12		
		13	6.3
		14	6.5
		15	6.8
		16	7.2
$R_1 =$	41.5	94.5	$= R_2$

Note where the values are the same and share the same rank, take an average of the rank values.

4. Total the ranks of each sample R_1 and R_2 (see the bottom of the table above).

5. Calculate the U values for both samples:

$$U_1 = k_1 k_2 + \frac{k_1(k_1 + 1)}{2} - R_1 = 58.5$$

$$U_2 = k_1 k_2 + \frac{k_2(k_2 + 1)}{2} - R_2 = 5.5$$

6. Use the table below to find the critical value for the U statistic at the $\alpha = 5\%$ level (or $p = 0.05$, the probability) for samples of this size ($k_1 = 8$ and $k_2 = 8$). Here α is the error rate that we are willing to accept

$$U_{crit} = 13$$

7. Reject the Null Hypothesis if the smallest value of U_1 or U_2 is below U_{crit} . In this case U_2 is below 13 we can reject the Null Hypothesis and accept the Alternative Hypothesis. The difference between the size of the bramble leaves in the light and the dark is significant for $P > 0.05$. Bramble leaves in the dark seem to be significantly bigger.

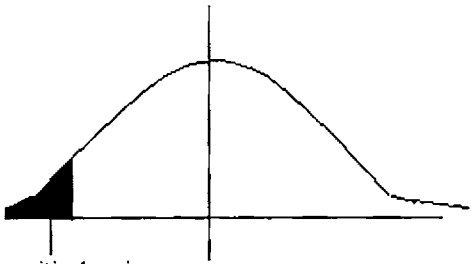
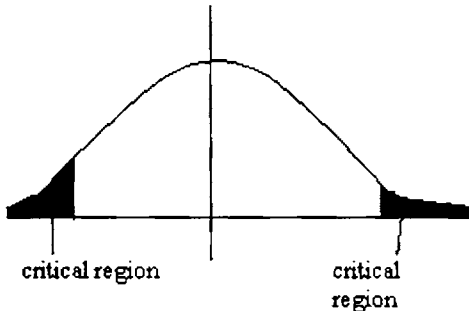
One and Two Tailed Tests

Suppose we have a null hypothesis H_0 and an alternative hypothesis H_1 . We consider the distribution given by the null hypothesis and perform a test to determine whether or not the null hypothesis should be rejected in favor of the alternative hypothesis.

There are two different types of tests that can be performed. A one-tailed test looks for an increase or decrease in the parameter whereas a two-tailed test looks for any change in the parameter (which can be any change- increase or decrease).

We can perform the test at any level (usually 1%, 5% or 10%). For example, performing the test at a 5% level means that there is a 5% chance of wrongly rejecting H_0 .

If we perform the test at the 5% level and decide to reject the null hypothesis, we say "there is significant evidence at the 5% level to suggest the hypothesis is false".

	
<p>One-Tailed Test</p>	<p>Two-Tailed Test</p>
<p>We choose a critical region. The critical region will have just one part (the shaded area above). If our sample value lies in this region, we reject the null hypothesis in favor of the alternative.</p>	<p>In a two-tailed test, we are looking for either an increase or a decrease. In this case, therefore, the critical region has two parts. If our sample value lies in this region, we reject the null hypothesis in favor of the alternative.</p>

Critical values of the Mann-Whitney U
(Two-Tailed Testing)

k2	α	k1																	
		3	4	5	6	7	8	9	10	11	12	13	14	15	16	17	18	19	20
3	.05		0	0	1	1	2	2	3	3	4	4	5	5	6	6	7	7	8
	.01		0	0	0	0	0	0	0	0	1	1	1	2	2	2	2	3	3
4	.05		0	1	2	3	4	4	5	6	7	8	9	10	11	11	12	13	14
	.01			0	0	0	1	1	2	2	3	3	4	5	5	6	6	7	8
5	.05	0	1	2	3	5	6	7	8	9	11	12	13	14	15	17	18	19	20
	.01			0	1	1	2	3	4	5	6	7	7	8	9	10	11	12	13
6	.05	1	2	3	5	6	8	10	11	13	14	16	17	19	21	22	24	25	27
	.01		0	1	2	3	4	5	6	7	9	10	11	12	13	15	16	17	18
7	.05	1	3	5	6	8	10	12	14	16	18	20	22	24	26	28	30	32	34
	.01		0	1	3	4	6	7	9	10	12	13	15	16	18	19	21	22	24
8	.05	2	4	6	8	10	13	15	17	19	22	24	26	29	31	34	36	38	41
	.01		1	2	4	6	7	9	11	13	15	17	18	20	22	24	26	28	30
9	.05	2	4	7	10	12	15	17	20	23	26	28	31	34	37	39	42	45	48
	.01	0	1	3	5	7	9	11	13	16	18	20	22	24	27	29	31	33	36
10	.05	3	5	8	11	14	17	20	23	26	29	33	36	39	42	45	48	52	55
	.01	0	2	4	6	9	11	13	16	18	21	24	26	29	31	34	37	39	42
11	.05	3	6	9	13	16	19	23	26	30	33	37	40	44	47	51	55	58	62
	.01	0	2	5	7	10	13	16	18	21	24	27	30	33	36	39	42	45	48
12	.05	4	7	11	14	18	22	26	29	33	37	41	45	49	53	57	61	65	69
	.01	1	3	6	9	12	15	18	21	24	27	31	34	37	41	44	47	51	54
13	.05	4	8	12	16	20	24	28	33	37	41	45	50	54	59	63	67	72	76
	.01	1	3	7	10	13	17	20	24	27	31	34	38	42	45	49	53	56	60
14	.05	5	9	13	17	22	26	31	36	40	45	50	55	59	64	67	74	78	83
	.01	1	4	7	11	15	18	22	26	30	34	38	42	46	50	54	58	63	67
15	.05	5	10	14	19	24	29	34	39	44	49	54	59	64	70	75	80	85	90
	.01	2	5	8	12	16	20	24	29	33	37	42	46	51	55	60	64	69	73
16	.05	6	11	15	21	26	31	37	42	47	53	59	64	70	75	81	86	92	98
	.01	2	5	9	13	18	22	27	31	36	41	45	50	55	60	65	70	74	79
17	.05	6	11	17	22	28	34	39	45	51	57	63	67	75	81	87	93	99	105
	.01	2	6	10	15	19	24	29	34	39	44	49	54	60	65	70	75	81	86
18	.05	7	12	18	24	30	36	42	48	55	61	67	74	80	86	93	99	106	112
	.01	2	6	11	16	21	26	31	37	42	47	53	58	64	70	75	81	87	92
19	.05	7	13	19	25	32	38	45	52	58	65	72	78	85	92	99	106	113	119
	.01	3	7	12	17	22	28	33	39	45	51	56	63	69	74	81	87	93	99
20	.05	8	14	20	27	34	41	48	55	62	69	76	83	90	98	105	112	119	127
	.01	3	8	13	18	24	30	36	42	48	54	60	67	73	79	86	92	99	105

Critical Values of the Mann-Whitney U
(One-Tailed Testing)

k2	α	k1																	
		3	4	5	6	7	8	9	10	11	12	13	14	15	16	17	18	19	20
3	.05	0	0	1	2	2	3	4	4	5	5	6	7	7	8	9	9	10	11
	.01		0	0	0	0	0	1	1	1	2	2	2	3	3	4	4	4	5
4	.05	0	1	2	3	4	5	6	7	8	9	10	11	12	14	15	16	17	18
	.01			0	1	1	2	3	3	4	5	5	6	7	7	8	9	9	10
5	.05	1	2	4	5	6	8	9	11	12	13	15	16	18	19	20	22	23	25
	.01		0	1	2	3	4	5	6	7	8	9	10	11	12	13	14	15	16
6	.05	2	3	5	7	8	10	12	14	16	17	19	21	23	25	26	28	30	32
	.01		1	2	3	4	6	7	8	9	11	12	13	15	16	18	19	20	22
7	.05	2	4	6	8	11	13	15	17	19	21	24	26	28	30	33	35	37	39
	.01	0	1	3	4	6	7	9	11	12	14	16	17	19	21	23	24	26	28
8	.05	3	5	8	10	13	15	18	20	23	26	28	31	33	36	39	41	44	47
	.01	0	2	4	6	7	9	11	13	15	17	20	22	24	26	28	30	32	34
9	.05	4	6	9	12	15	18	21	24	27	30	33	36	39	42	45	48	51	54
	.01	1	3	5	7	9	11	14	16	18	21	23	26	28	31	33	36	38	40
10	.05	4	7	11	14	17	20	24	27	31	34	37	41	44	48	51	55	58	62
	.01	1	3	6	8	11	13	16	19	22	24	27	30	33	36	38	41	44	47
11	.05	5	8	12	16	19	23	27	31	34	38	42	46	50	54	57	61	65	69
	.01	1	4	7	9	12	15	18	22	25	28	31	34	37	41	44	47	50	53
12	.05	5	9	13	17	21	26	30	34	38	42	47	51	55	60	64	68	72	77
	.01	2	5	8	11	14	17	21	24	28	31	35	38	42	46	49	53	56	60
13	.05	6	10	15	19	24	28	33	37	42	47	51	56	61	65	70	75	80	84
	.01	2	5	9	12	16	20	23	27	31	35	39	43	47	51	55	59	63	67
14	.05	7	11	16	21	26	31	36	41	46	51	56	61	66	71	77	82	87	92
	.01	2	6	10	13	17	22	26	30	34	38	43	47	51	56	60	65	69	73
15	.05	7	12	18	23	28	33	39	44	50	55	61	66	72	77	83	88	94	100
	.01	3	7	11	15	19	24	28	33	37	42	47	51	56	61	66	70	75	80
16	.05	8	14	19	25	30	36	42	48	54	60	65	71	77	83	89	95	101	107
	.01	3	7	12	16	21	26	31	36	41	46	51	56	61	66	71	76	82	87
17	.05	9	15	20	26	33	39	45	51	57	64	70	77	83	89	96	102	109	115
	.01	4	8	13	18	23	28	33	38	44	49	55	60	66	71	77	82	88	93
18	.05	9	16	22	28	35	41	48	55	61	68	75	82	88	95	102	109	116	123
	.01	4	9	14	19	24	30	36	41	47	53	59	65	70	76	82	88	94	100
19	.05	10	17	23	30	37	44	51	58	65	72	80	87	94	101	109	116	123	130
	.01	4	9	15	20	26	32	38	44	50	56	63	69	75	82	88	94	101	107
20	.05	11	18	25	32	39	47	54	62	69	77	84	92	100	107	115	123	130	138
	.01	5	10	16	22	28	34	40	47	53	60	67	73	80	87	93	100	107	114